

Model for nonleptonic and semileptonic decays by $\bar{B}^0 \rightarrow D^{**}$ transitions with $\text{BR}(j=1/2) \ll \text{BR}(j=3/2)$ using the Leibovich-Ligeti-Stewart-Wise scheme

Alain Le Yaouanc,^{*} Jean-Pierre Leroy,[†] and Patrick Roudeau[‡]
Université Paris-Saclay, CNRS/IN2P3, IJCLab, 91405 Orsay, France

 (Received 5 June 2021; accepted 29 November 2021; published 6 January 2022)

We present a model for the vector and axial form factors of the transitions $\bar{B}^0 \rightarrow D^{**}$ in good agreement with the presently available data and based on the present theoretical knowledge, combining (a) the safe lattice QCD predictions at $m_Q = \infty$ and $w = 1$; (b) the predictions at general w of a relativistic, covariant quark model at $m_Q = \infty$, including the well-tested Godfrey and Isgur spectroscopic model and which agrees with lattice QCD at $w = 1$; (c) the constraint of Bjorken and Neubert relating semileptonic and class I nonleptonic decays, which shows that $\bar{B}^0 \rightarrow D_0(2300)^+ \pi^-$ strongly constrains $\tau_{1/2}(w)$ to be much smaller than $\tau_{3/2}(w)$, in agreement with the theoretical expectation; and (d) the general HQET expansion which constrains the $1/m_Q$ corrections (cf. Leibovich *et al.* *Phys. Rev. Lett.* **78**, 3995 (1997)., denoted hereafter as LLSW). An important element in the understanding of data is the large contribution of virtual $D_V^{(*)}$ to the broad structures seen in SL decays at low $D^{(*)}\pi$ masses—which makes it difficult to isolate the broad resonances denoted as $D_{1/2}$ in the following.

DOI: [10.1103/PhysRevD.105.013004](https://doi.org/10.1103/PhysRevD.105.013004)

I. INTRODUCTION

There is insufficient knowledge of both nonleptonic (NL) and semileptonic (SL) transitions to charmed orbital excitations, generically termed as D^{**} .¹ The latter (SL) are especially interesting: (1) in themselves, for (a) striking theoretically expected features which contradict the naive idea of a strong similarity between SL transitions to $j = 1/2$ and $j = 3/2$ D^{**} , and (b) for the apparent contradiction between this expectation and the presently widespread interpretation of experimental data on broad states, a contradiction which we claim to have resolved by the interplay of the possibly large D_V^* background [2]. (2) For some applications, like the background to $\bar{B} \rightarrow D^{(*)} \ell^- (\tau^-) \bar{\nu}_{\ell(\tau)}$. Ultimately, one would like to have a description of the full system of semileptonic $\bar{B} \rightarrow D^{**}$ form factors, but this appears to be a hard task.

^{*}alain.le-yaouanc@ijclab.in2p3.fr

[†]jean-pierre.leroy@ijclab.in2p3.fr

[‡]patrick.roudeau@ijclab.in2p3.fr

¹We generically use the notation D^{**} , as is done in [1], to refer to the four lightest excited D mesons whenever it is not necessary to distinguish between them. Similarly, $D^{**,+}$ (respectively $D^{**,0}$) denotes the positive (respectively neutral) states.

Published by the American Physical Society under the terms of the Creative Commons Attribution 4.0 International license. Further distribution of this work must maintain attribution to the author(s) and the published article's title, journal citation, and DOI. Funded by SCOAP³.

Indeed, there are no full calculations of the latter from first principles, as are provided in simpler cases by lattice QCD. Presently, the latter gives results only at $m_Q = \infty$ and $w = 1$. The reasons are given below in Sec. II.

On the other hand, the experimental data are scarce: total branching ratios, some points in the $d\Gamma/dw$ of certain transitions, etc. Then, as explained in more detail in Secs. II and VIII, a more complicated path is to be followed, combining theoretical inputs and experience, the former being used in several different ways.

We indeed want to use the very useful general ideas of the extensive analyzes of [3–5],² relying on their HQET analysis, but we take into account the following: (1) quantitative dynamical results at $m_Q = \infty$ of lattice QCD [completed by quark models in the Bakamjian-Thomas (BT) approach] as well as (2) the very important experimental measurements of $\bar{B}^0 \rightarrow D_0(2300)^+ \pi^-$, which strongly constrain the transition to $j = 1/2$ to be small. Both of these have been disregarded in the LLSWB analyses.

Finally, we underline the very important role of the D_V^* background in the SL decays, which we have already emphasized in [2]. We believe this role has not been fully taken into account up to now.

²From now on, we refer to this set of analyses as LLSWB. When comparing such types of analyses with our model, we use the acronym LLSWB*i* where the “i” means “inspired,” implying slight modifications to LLSWB are required for a fair comparison with our own model, as explained in Appendix D.

All these elements, taken together, drastically change the conclusions with respect to the ones of the above-mentioned analyses, especially the fact that the Isgur-Wise (IW) functions (see Sec. II A) are roughly equal at $w = 1$, as we explain now.

The LLSW approach [3] provides a framework to parametrize $1/m_Q$ corrections in corresponding hadronic form factors and applies factorization to relate semileptonic and class I nonleptonic decays. Such analyses [4,5], which take as input quoted values [6,7] for $\bar{B}^0 \rightarrow D^{**,+} \ell^- \bar{\nu}_\ell$, conclude that the production of narrow and broad D^{**} states is similar. Meanwhile, to reach this conclusion, one has to discard the measurement of $\bar{B}^0 \rightarrow D_0(2300)^+ \pi^-$,³ which implies, as a consequence of factorization, a very small value for the production of the $D_0(2300)$ meson in semileptonic decays, when compared with the rates measured for narrow states. This might be justified because such a low value, evaluated for $\bar{B}^0 \rightarrow D_0(2300)^+ \ell^- \bar{\nu}_\ell$, appears to be in contradiction with the rates measured in experiments for this channel. However, we think that the nonleptonic data for the $D_{1/2}$ are much more trustable than the semileptonic ones. Indeed, the identification of the $D_0(2300)$ in the nonleptonic channel is supported by (1) the extraction of D_V^* and (2) the measurement of the phase shift, while no such work has been done in the semileptonic case (except, for D_V^* , the work reported in [8]). Moreover, from a theoretical point of view, the smallness of the transitions to the $D_{1/2}$ states with respect to the $D_{3/2}$ ones has initially been anticipated using quark models and, later, by direct LQCD evaluations.

We consider this problem again and propose a model, also based on the LLSW parametrization, which uses all the measured nonleptonic class I decays in the framework of factorization. This model agrees with LQCD and relativistic quark model (RQM) expectations. Because, in this model, production of broad D^{**} mesons is expected to be much smaller than the production of narrow states, it is necessary to add another broad component to be able to explain the broad mass distributions measured in $\bar{B}^0 \rightarrow D^{(*)} \pi \ell^- \bar{\nu}_\ell$ decays. We find that $D_V^{(*)}$ decays can fill such a gap. In the following, we detail our model and provide comparisons with the LLSWBi model in which the broad

$D^{(*)} \pi$ mass distributions are explained by the contributions from D^{**} decays alone, as done in previous analyses where the measurement from $\bar{B}^0 \rightarrow D_0(2300)^+ \pi^-$ is not used.

Finally, one is led to a solution with a $j = 1/2$ rate much smaller than the $j = 3/2$ one.

II. THEORETICAL INPUTS

We mention “inputs” because one lacks a systematical theoretical treatment: rather, one uses a mixture of procedures, including the very experimental data which are to be explained, and fitting.

In addition, several ingredients [(a)–(d), as enumerated in the abstract] are available.

We can classify them into two categories, as follows.

A. Dynamical results at $m_Q = \infty$

In the infinite quark mass limit, hadronic form factors that describe $\bar{B} \rightarrow D^{**}$ are determined by the two Isgur-Wise functions: $\tau_{3/2}(w)$ and $\tau_{1/2}(w)$. Their values at $w = 1$ and their w dependence are constrained by two types of theoretical considerations. The first come from lattice QCD for $w = 1$ at $N_F = 0, 2$; at $N_F = 2$ [9]

$$\tau_{3/2} = 0.526 \pm 0.023, \quad \tau_{1/2} = 0.296 \pm 0.026 \quad (1)$$

showing a striking difference between them, in contrast to a naive nonrelativistic (NR) expectation, according to which these two quantities are equal.

These are trustable results which cannot be disregarded. In the most recent simulation the lattice spacing is reasonably small, $a = 0.085$ fm, and the volume is reasonably large, $24^3 \times 48$, although certain systematic errors are not estimated. Of course, these results should be improved. One notes that, at $N_F = 2$, the inequality between $j = 1/2$ and $j = 3/2$ values is appreciably reinforced with respect to the older $N_F = 0$ ones. The second ones stem from quark models, which, although purely phenomenological, have the advantage of providing results for $w \neq 1$ as well.

Of course, there are a very large variety of quark models. We consider a class of models for current matrix elements where the calculation is decomposed into two steps: (1) the determination of the wave functions at rest and (2) a procedure to derive the state in motion. Then, there are a variety of spectroscopic models, describing the spectrum and the wave functions at rest, i.e., internal quark motion; another variety comes from the way one describes the hadron motion.

Among the many spectroscopic models, we use an outstanding one by Godfrey and Isgur (GI) [10]. This model is unique in that it covers a very large number of hadronic states, both with light quarks and with heavy ones. One must underline the fact that most predictions have been confirmed by later experiments. Although it is a

³In fact, in the first two papers [1] and [3], the NL decays were not used to constrain the semileptonic ones, and anyway, $\bar{B}^0 \rightarrow D_0(2300)^+ \pi^-$ has not yet been measured. In [4] and [5], on the other hand, $\bar{B}^0 \rightarrow D_0(2300)^+ \pi^-$ was known, and in [4], it was considered to be “puzzling.” Indeed, one can see that the measured value would clearly contradict, through factorization, their fit to $\bar{B}^0 \rightarrow D_0(2300)^+ \ell^- \bar{\nu}_\ell$, near w_{\max} , by an order of magnitude (see the comparison of the experimental number and the LLSWBi value in Table XII), while the agreement is quite good for the fit to $\bar{B}^0 \rightarrow D_2^{*+} \ell^- \bar{\nu}_\ell$. Finally, in [5], $\bar{B}^0 \rightarrow D_0(2300)^+ \pi^-$ data were explicitly discarded: only $\bar{B} \rightarrow D_{3/2} \pi$'s are used (see the beginning of their Sec. IV, p. 9).

complicated model with many parameters, the latter can be determined because the model covers of a very extended spectrum. This model has a relativistic kinetic energy, and its success confirms the necessity of a relativistic treatment of quark internal motion inside hadrons, which is already implied by the fact that excitation energies are of the order of the reduced mass.

For the description of hadron motion, we use a specific framework, the one of Bakamjian and Thomas, to describe states in relativistic motion at $m_Q = \infty$. It has several advantages:

- (i) it uses the standard three-dimensional wave functions at rest provided by spectroscopic models;
- (ii) it is relativistic as to hadronic motion, and even covariant;
- (iii) it satisfies the standard set of HQET sum rules, like Bjorken [11] and curvature [12] sum rules, Uraltsev sum rules [13], etc.

The last two points are important advantages compared to the nonrelativistic treatment of quark motion, even if we were adopting the GI spectroscopic model. Note that a NR treatment of hadron motion is not satisfactory for the full range of w since the 3-velocity at w_{\max} is large even in the “equal velocity frame” which minimizes velocities: $v = \sqrt{(w-1)/2} \simeq 0.4$.

Moreover, these differences lead to quite different quantitative results. In the NR quark models with non-relativistic treatment of both internal quark velocities and hadron motion, a general statement⁴ would be

$$\tau_{1/2}(w) = \tau_{3/2}(w), \quad (2)$$

in clear contradiction with the above lattice QCD results. The equality (2) assumes that there is no sizable spin-orbit force surviving at $m_Q = \infty$, which is not a theorem but seems reasonable from the spectroscopic model studies and leads to identical rest-frame wave functions.

In the BT framework, using the well-known spectroscopic model of GI [10], one finds very different values for $j = 1/2$ and $j = 3/2$ [15]:

$$\tau_{3/2}(1) \simeq 0.5, \quad \tau_{1/2}(1) \simeq 0.25, \quad (3)$$

in full agreement with QCD. This strikingly large difference is a general feature of the BT approach, which provides an intuitive explanation: it is due to the typically relativistic effect of Wigner rotations of spin, included in

⁴In Ref. [14], the calculation is done for harmonic oscillator wave functions, but this does not alter the generality of the conclusion. Note also that a “relativisation” factor κ has to be disregarded in their Eq. (44). Possible additional factors expressed as powers of $(w+1)/2$ encountered in the literature must also be disregarded since such factors give a 1/2 contribution to the slope while the dominant NR approximation gives a slope that goes $\rightarrow \infty$ as $m^2 R^2$ [see Eq. (44) of [14]].

the BT approach, which acts differently on $j = 3/2$ and $j = 1/2$ states in motion and which is completely independent of the presence of possible spin-dependent forces in the potential.

Note that there is an important sum rule by Uraltsev concerning the difference between $j = 3/2$ and $j = 1/2$, with transitions to all excited states included:

$$\sum_n (|\tau_{3/2}^{(n)}(1)|^2 - |\tau_{1/2}^{(n)}(1)|^2) = 1/4. \quad (4)$$

This shows that the sum over n : $\sum_n |\tau_{3/2}^{(n)}(1)|^2$ is much larger than the one concerning 1/2 states: $\sum_n |\tau_{1/2}^{(n)}(1)|^2$. If one assumes that the transitions to radial excitation are sufficiently small, this would imply that $|\tau_{3/2}^{(0)}| > |\tau_{1/2}^{(0)}|$, in agreement with Eq. (3). See the extensive discussions by Bigi *et al.* [16]; see also [17] and the work on zero-recoil sum rules of [18] and [19]. In the latter reference, the point of view of the authors on this matter is expressed at the end of Sec. 6.3.2. However, the argument is, of course, not compelling.

In summary, considering the lattice result (1), one should estimate that the marked difference between $\tau_{3/2}(1)$ and $\tau_{1/2}(1)$ is a firmly established result. It is moreover supported by the above-mentioned physical argument provided by the role of Wigner rotations in the quark model. Finally, as we shall see later, using factorization, the nonleptonic decays $\bar{B} \rightarrow D^{**}\pi$ tend to the same conclusion for $q^2 \simeq 0$ or $w \simeq 1.35$. Combined with the appropriate kinematical factors and converted into branching ratios, this leads to the still-more-striking inequality

$$\mathcal{B}(\bar{B}^0 \rightarrow D_{1/2}) \ll \mathcal{B}(\bar{B}^0 \rightarrow D_{3/2}) \quad (5)$$

by around 1 order of magnitude, and we claim to provide a model which both satisfies this strong inequality and fits the data well.⁵

The quantitative agreement of the BT prediction with the lattice QCD one gives encouragement to trust the predicted shapes at $w \neq 1$, another crucial theoretical input.

The full shape is well approximated by a relativistic quark-model-inspired description [21]:

$$\tau_{3/2(1/2)}(w) = \tau_{3/2(1/2)}(1) \times \left(\frac{2}{w+1} \right)^{2\sigma_{3/2(1/2)}}. \quad (6)$$

Numerically,

$$\sigma_{3/2}^2 \simeq 1.5, \quad \sigma_{1/2}^2 \simeq 0.8. \quad (7)$$

These values are in contrast with what would be given in a fully NR treatment, namely, a common and much lower

⁵The strong inequality between the branching ratios is also clearly seen in Table III of [20].

value, of order 0.4 (obtained from [14] and skipping the relativisation factor κ).

Other analyses use instead a linear approximation for the τ -functions: $\tau_i(w) = \tau_i(1) \times (1 - \sigma_{i,\text{lin}}^2(w-1))$. It can be checked that $\sigma_{i,\text{lin}}^2 = \sigma_i^2$ when $w = 1$. In practice, the two descriptions are rather similar because the w variation range, between 1 and $w_{\text{max}} = (m_B^2 + m_{D^{**}}^2)/(2m_B m_{D^{**}})$, is limited anyway. Meanwhile, significant differences are expected from the two parametrizations when comparing semileptonic decays with a light or a heavy lepton, as evaluated in Table XIII.

Why start from $m_Q = \infty$? The visible difficulty is that one presently has trustable quantitative statements only for $m_Q = \infty$. The reasons for this are as follows: (1) for lattice QCD, it is very difficult to directly treat the finite masses m_b, m_c , all the more for transitions to excitations. Thus, one uses an $m_Q = \infty$ framework. Then, to treat finite $w \neq 1$, one would require infinite momenta, whence one is restricted to $w = 1$. (2) Quark models, in general, have no such limitations. However, the BT framework we want to use is satisfactory only at $m_Q = \infty$. Indeed, it has been shown that the finite mass corrections cannot be trusted: they break covariance as well as certain important sum rules, in contrast with the $m_Q = \infty$ limit. This defect remains to be resolved.

The consequence is that these dynamical results must be complemented by other statements, of a more general nature, which provide constraints on the physical transitions (of course, at finite mass) or, equivalently, on finite mass corrections to the above dynamical results. These questions are considered below.

B. Use of general statements or relations

First, we rely on the validity of the factorization, as does, in principle, LLSWB. This phenomenon has been firmly established from the theoretical point of view, within perturbative QCD, in the heavy quark asymptotic limit $m_Q \rightarrow \infty$ (from the successive efforts of Dugan and Grinstein [22], BBNS [23], and finally, Bauer, Pirjol, and Stewart [24]), with the high precision NNLO result of the Siegen group [25], $a_1^\infty = 1.07 \pm 0.022$, which is therefore higher but not far from the naive $a_1 = 1$.

Of course, since QCD factorization only gives an asymptotic statement, a departure from this limit is quite expected [the presence of various $(1/m_Q)^n$ corrections extensively discussed in BBNS, m_c not very large, etc.], although this departure cannot be estimated quantitatively. Moreover, the moderate order of magnitude of the departure from asymptotic BBNS factorization, [$a_1 = 1 + \mathcal{O}(10\%)$] for a number of well-measured decays as observed from the experimental side, is such that it does not seem possible to doubt its approximate validity for the decays which we are presently studying.

Factorization implies Bjorken's relation [26]⁶ between the NL and SL decays at some q^2 (for example, m_π^2 for decay by pion emission), which is a very strong and useful constraint for the otherwise ill-known SL differential q^2 distributions.

Practically, since we have no theoretical quantitative estimates of the departure of a_1 from the asymptotic BBNS result, we will apply factorization in the following way. We fit a_1^{eff} in $\bar{B} \rightarrow D(3/2)$ decays and find a value compatible with those obtained by analyzing $\bar{B} \rightarrow D^{(*)}$ transitions (see Sec. VI). Then, in our final analysis, we impose a constraint in the fits: $a_{1\text{eff}} = 0.93 \pm 0.07$. This a_1^{eff} will also be used for cases where experimental data are lacking or not precise enough. This procedure is, in principle, valid for class I decays with emission of a light meson. But we shall extend it to predict NL processes where a charmed strange meson is emitted like $B \rightarrow D^{**} D_s^{(*)}$; although in such a case the asymptotic theorem of BBNS does not apply, one again obtains a value of a_1^{eff} close to 1 from the measured processes.

Secondly, let us comment about HQET and $1/m_Q$ expansion. The constraints from HQET expansion as performed in [3] and further work, including order $\mathcal{O}(1/m_Q)$ corrections, are crucial, too, as a necessary complement to the $m_Q = \infty$ predictions.

For the determination of the $\mathcal{O}(1/m_Q)$ subdominant functions, one must stress that the constraints do not lead to quantitative statements on the finite mass corrections; rather, they yield a parametrization of these finite corrections. They leave us with a large number of unknown parameters and functions of w . Some of these parameters, like $\bar{\Lambda}$ (quoted as set 1 in the following), can be estimated otherwise, as explained in Sec. II C. One could think of fixing the remaining unknown parameters (set 2) by fits to the experimental data. But there remains at least a host of unknown functions of w . For instance, for $j = 3/2$, one needs, in principle, the ten functions: $\tau_1(w), \tau_2(w), \eta_{\text{ke}}^{b,c}(w), \eta_{1,2,3}^{b,c}(w)$ in LLSW notation,⁷ which is of course too large a number to be fitted at present. This number is reduced thanks to the fact that the η_i^b 's and η_{ke}^b are present only in one combination, $\eta^b = \eta_{\text{ke}}^b + 6\eta_1^b - 2\eta_2^b(w-1) + \eta_3^b$, but the problem remains.

Many further assumptions must then be added: (1) an additional but reasonable assumption of rough proportionality of the latter functions to the dominant Isgur-Wise functions reduces them to numerical parameters, denoted with ‘‘hats,’’ but one still has a host of unknown numbers.

⁶Popularized by Neubert [27]. As stressed by Neubert, the principle of this relation dates back to Bjorken, who applied it to the case of $\Lambda_b \rightarrow p\pi$ decay [see his Eq. (4.5)] and referred also to the pionic B decays. Neubert applied it to the decays into D^{**} and generalized it to arbitrary values of a_1 .

⁷Be careful not to confuse the subindices to τ 's (1,2) with the previous subindices $j = 1/2, 3/2$ concerning the dominant Isgur-Wise functions.

For $D_{3/2}$ mesons, present data are sensitive to the values of $\hat{\eta}_{1,3}$ and $\hat{\tau}_1$, which we have determined, while some guesses have to be used to define a possible range of variation for the other two quantities: $\hat{\eta}_2$ and $\hat{\tau}_2$. For $D_{1/2}$ mesons, data are much less accurate, and fits have the same sensitivity to $\hat{\chi}_{1,2}$ or $\hat{\xi}_1$; one can obtain the value for only one of these quantities. We arbitrarily choose to fit $\hat{\chi}_1$.

However, one would like to find some reasons for that selection or consistency checks for the physical soundness of the values of the parameters found in this way.

LLSW [1] proposed an additional expansion in $w - 1$ (the latter being too small, of magnitude at most $\simeq 0.3 \simeq \epsilon_c = 1/2m_c$) in the narrow width approximation ($w_{\max} \simeq 1.3$, $m_c \simeq 1.5$ GeV). Were this valid, it would allow us to skip $\tau_{1,2}$ terms as being of higher order and to be left with the η 's. However, this supposes that the $\tau_{1,2}$ are not large, a point for which there is no guarantee (in fact, one often retains the reverse, i.e., dropping the η 's in favor of the $\tau_{1,2}$). In the present analysis we have not used any expansion in $w - 1$, and we take the full $1/m_Q$ expansions of the Lorentz invariant form factors given in [3]. The validity of this framework requires that unknown quantities that enter in the expansion are of order $\bar{\Lambda}$. This is what we verify for fitted quantities; therefore, we have assumed that quantities, not determined by the fit, are also of that order to evaluate their contribution to systematic uncertainties.

Inspiration from quark models can help one check the soundness of fit results, at least qualitatively. As explained above, one cannot trust the BT approach for finite mass corrections, and this is the main obstacle to getting physical results in this quark model approach. Then, one may return to the NR model of center-of-mass motion, but only to get a qualitative understanding. An example is the η functions, which correspond, in naive terms, to the modification of the wave functions induced by the change of m_Q from ∞ to its real value in the Schrödinger equation.

Knowing, theoretically, the “true” (infinite mass) $\tau_{3/2}(w = 1)$, the magnitude of the corrections at $w = 1$, which appear in the combination $\frac{\eta^b}{2m_b} + \frac{\eta_{\text{ke}}^c}{2m_c}$ (corresponding to our $\hat{\epsilon}_{3/2}$ below), can be rather well determined with a stable value in the various fits to the data, and it is found to be unambiguously negative.

A fully NR calculation of the effect of $\mathcal{O}_{\text{ke}}(v = (1, 0, 0, 0))$ (naively interpreted as the effect of the change of the kinetic energy on the wave functions in the rest frame) suggests a negative $\eta_{\text{ke}}^c(w = 1)$ corresponding to the effect on the final state. On the contrary, η_{ke}^b should be positive, but the combination η^b corresponds to the total effect on the state vectors, including $\mathcal{O}_{\text{mag}}(v = (1, 0, 0, 0))$, and, naively interpreted, includes the large spin-spin force present at finite mass. In the GI model, it is found to be neatly negative by numerical calculation.

Then, it is encouraging to find consistency between the theoretically expected sign and the finding of the fits. One could hope to similarly estimate the signs and order of magnitude of the remaining η_i^c 's, but this requires interpreting them separately in the quark model (see Appendix B).

On the whole, at present, there is no theoretical estimate for the values of the different parameters that enter in the LLSW expansion, except, perhaps, a qualitative one of the η 's if we follow the arguments above (see also Appendix B).

C. Evaluation of HQET parameters

In the framework of HQET, masses of charm and beauty mesons are used to evaluate values of the parameters (named set 1 in the following) that enter in some of the $1/m_Q$ corrections [3], the relation being

$$m_{H_{\pm}} = m_Q + \bar{\Lambda}^H - \frac{\lambda_1^H}{2m_Q} \pm \frac{n_{\mp} \lambda_2^H}{2m_Q} + \dots \quad (8)$$

The total spin (J_{\pm}) of the resonance (H_{\pm}) is expressed in terms of the total spin (s_l) of the light hadronic system as $J_{\pm} = s_l \pm 1/2$, while $n_{\pm} = 2J_{\pm} + 1$ is the number of spin states. Values of these different quantities and those of meson masses, adopted in our analysis, are indicated in Table I. We do not consider I-spin averaged masses and use only charged ($c\bar{d}$) states for charm and neutral states for beauty ($b\bar{d}$).

We use, for $\bar{\Lambda}^H$, the notations $\bar{\Lambda}$, $\bar{\Lambda}_{3/2}$, and $\bar{\Lambda}_{1/2}$ for the s_l^{π} doublets $1/2^-$, $3/2^+$, and $1/2^+$ respectively.

Considering only the first order expansion in $1/m_Q$ of Eq. (8), the ratio (r_Q) between charm and beauty quark masses is equal to

$$r_Q = \frac{m_c}{m_b} = \frac{m_{B^*} - m_B}{m_{D^*} - m_D} = 0.3215 \pm 0.0015. \quad (9)$$

The difference between the $\bar{\Lambda}^H$ values for the three doublets can be expressed in terms of the ratio between heavy quark masses and the values of spin averaged masses (\bar{m}) [3]. We have obtained

TABLE I. The three doublets of heavy mesons, which have, respectively, a total spin and parity of their light component s_l^{π} equal to $1/2^-$, $3/2^+$, and $1/2^+$. The masses are given in MeV.

Meson	J^P	s_l^{π}	n_{\pm}	Charm mass	Beauty mass
D^+/\bar{B}^0	0^-	$1/2^-$	$n_- = 1$	1869.65 ± 0.05	5279.65 ± 0.12
D^{*+}/\bar{B}^{*0}	1^-	$1/2^-$	$n_+ = 3$	2010.26 ± 0.05	5324.70 ± 0.21
D_1^+/B_1^0	1^+	$3/2^+$	$n_- = 3$	2423.8 ± 1.1	5726.1 ± 1.4
D_2^{*+}/B_2^{*0}	2^+	$3/2^+$	$n_+ = 5$	2465.4 ± 1.3	5739.5 ± 0.7
$D_0(2300)^+$	0^+	$1/2^+$	$n_- = 1$	2330 ± 20	unmeasured
$D_1(2430)^+$	1^+	$1/2^+$	$n_+ = 3$	$2452 \pm (?)$	unmeasured

TABLE II. Values of HQET parameters used in the evaluation of $1/m_Q$ corrections (first line). The last line gives the values used in previous analyses. The various quantities are expressed in GeV, except for λ_1 (GeV²).

λ_1	$\bar{\Lambda}$	$\bar{\Lambda}_{3/2}$	$\bar{\Lambda}_{1/2}$	m_c	m_b
-0.362	0.245	0.641	0.611	1.618	5.032
-0.2	0.4	0.8	0.76	1.4	4.8

$$\bar{\Lambda}_{3/2} - \bar{\Lambda} = (396.0 \pm 1.5) \text{ MeV.} \quad (10)$$

For the $1/2^+$ doublet the corresponding estimate is more uncertain because the associated B -meson states are still unmeasured. From the masses of charm states we estimate $\bar{\Lambda}_{1/2} - \bar{\Lambda} \sim 366 \text{ MeV}$.

These values for $\bar{\Lambda}_{3/2} - \bar{\Lambda}$ and $\bar{\Lambda}_{1/2} - \bar{\Lambda}$ agree with previous determinations.

To evaluate absolute values for heavy quark masses and $\bar{\Lambda}$, one needs a value for λ_1 . In previous analyses, the value $\lambda_1 = -0.2 \text{ GeV}^2$ was used; in a recent report from the HFLAV Collaboration [6], the value $\lambda_1 = (-0.362 \pm 0.067) \text{ GeV}^2$ was obtained from an analysis of B -meson semileptonic decays. In Table II a summary is given for the values of the different parameters entering in the analysis [first line, with $\lambda_1 = -0.362 \text{ (GeV}^2\text{)}^2$].

D. Evaluation of parameters entering in the LLSW parametrization

In the infinite quark mass limit, hadronic form factors that describe $\bar{B} \rightarrow D^{**}$ are determined by the two Isgur-Wise functions: $\tau_{3/2}(w)$ and $\tau_{1/2}(w)$, respectively, which have been introduced in Eq. (6). It has been noted [3] that one can define useful effective functions including finite mass corrections to replace the IW functions: namely, particularizing at $w = 1$, one writes

$$\begin{aligned} \tau_{3/2}^{\text{eff}}(1) &= \tau_{3/2}(1) + \frac{\eta_{\text{ke}}(1)}{2m_c} + \frac{\eta_b(1)}{2m_b} = \tau_{3/2}(1) \times |1 + \hat{e}_{3/2}|, \\ \tau_{1/2}^{\text{eff}}(1) &= \tau_{1/2}(1) + \frac{\chi_{\text{ke}}(1)}{2m_c} + \frac{\chi_b(1)}{2m_b} \\ &= \tau_{1/2}(1) \times |1 + \hat{e}_{1/2}|. \end{aligned} \quad (11)$$

In Table III we give the parameters that enter in the expressions of Lorentz-invariant form factors for the LLSW parametrization of $\bar{B} \rightarrow D^{**}$ transitions.

III. $\bar{B}^0 \rightarrow D^{**}$ EXPERIMENTAL RESULTS USED AS CONSTRAINTS

Input data, in this analysis, are obtained by averaging branching fraction measurements of nonleptonic class I, $\bar{B}^0 \rightarrow D^{**,+} \pi^- (K^-)$, and semileptonic decay $\bar{B} \rightarrow D^{**} \ell^- \bar{\nu}_\ell$ channels. These last values, obtained separately for charged

TABLE III. List of the parameters that enter in the LLSW formalism. The last two columns indicate how values of these quantities are obtained in the present analysis. When no information is available on a parameter, it is set to zero, and a range of $\pm 0.5 \text{ GeV} \sim \pm \bar{\Lambda}$ is used to evaluate a plausible contribution to systematic uncertainties.

	Parameters list	Evaluation	Constraints from theory
Set 1	$m_{b,c}, \bar{\Lambda}, \bar{\Lambda}_{3/2}, \bar{\Lambda}_{1/2}$	Using HQET	See Sec. II C
Set 2 for $D_{3/2}$ mesons	$\tau_{3/2}(1)$ $\hat{e}_{3/2}$ $\sigma_{3/2}^2$ $\hat{\eta}_{1,3}, \hat{\tau}_1$ $\hat{\eta}_2, \hat{\tau}_2$	Fitted Fitted Fitted Fitted Set to zero	0.53 ± 0.03 1.5 ± 0.5 $\pm 0.5 \text{ GeV}$
Set 2 for $D_{1/2}$ Mesons	$\tau_{1/2}^{\text{eff}}(1)$ $\sigma_{1/2}^2$ $\hat{\chi}_1$ $\hat{\chi}_2, \hat{\zeta}_1$	Fitted Fitted Fitted Set to zero	0.20 ± 0.06 $\sigma_{3/2}^2 - \sigma_{1/2}^2 = 0.7 \pm 0.5$ $\pm 0.5 \text{ GeV}$

and neutral B mesons, are combined, assuming the equality of corresponding partial decay widths for charged and neutral B mesons, and averaged values are expressed in terms of the \bar{B}^0 . We have taken into account possible correlations between the different uncertainties, corrected intermediate branching fractions [7], and used the hypotheses explained in Sec. III A to evaluate D^{**} absolute decay branching fractions. Values obtained in this way are compared with those used in a previous analysis [4] in Table IV. The first lines are relative to the production of narrow ($D_{3/2}$) states; then, they correspond to broad ($D_{1/2}$) states, and the last line reports a ratio between the production of narrow and broad states. Therefore, apart from the last constraint, it is possible to investigate the production of narrow and broad states, independently.

Production of $D_{1/2}$ mesons in semileptonic decays, reported in the last two columns of Table IV, is derived from HFLAV [6], whereas that used in our analysis is obtained using a different approach, as explained in Sec. III B. As illustrated from the values given in Table IV and from the results of the fits quoted in Tables XIII and XVIII, estimates for $D_1(2430)$ are not accurate, with about 100% uncertainty, after taking into account the fact that existing measurements are rather incompatible, with $\chi^2/NDF = 18/2$, and if we scale the uncertainty, obtained on the average value, using the ‘‘PDG recipe’’ that corresponds to a factor of 3. Such a scaling factor is not included in the [4] analysis, and the present value from PDG [$\sim (4 \pm 1) \times 10^{-3}$], not quoted in Table IV, is based on the measurement from *BABAR* alone, not including the other two results that enter in the HFLAV average, and which are rather different—in particular, the one from Belle, which does not see a signal and quotes a stringent limit.

TABLE IV. Measured branching fractions used as constraints in the present analysis. In the last two columns we indicate the values used in a previous analysis and those quoted in PDG [7] or obtained by HFLAV [6]. As compared with our numbers, these values differ mainly in the estimate of the production of broad D^{**} states in B -meson semileptonic decays. The analysis [4] also differs by the fact that nonleptonic measurements of $D_{1/2}$ states are not included.

Decay channel	This analysis	Analysis [4] (2016)	PDG (2020) or HFLAV ^c
$\mathcal{B}(\bar{B}^0 \rightarrow D_2^{*+} \pi^-) \times 10^4$	5.85 ± 0.42	5.9 ± 1.3	5.85 ± 0.43
$\mathcal{B}(\bar{B}^0 \rightarrow D_2^{*+} K^-) \times 10^5$	4.7 ± 0.8	Not used	5.0 ± 0.9
$\mathcal{B}(\bar{B}^0 \rightarrow D_2^{*+} \ell^- \bar{\nu}_\ell) \times 10^3$	3.09 ± 0.32	2.8 ± 0.4	3.18 ± 0.26
$\mathcal{B}(\bar{B}^0 \rightarrow D_1^+ \pi^-) \times 10^4$	7.12 ± 1.13	7.5 ± 1.6	6.6 ± 2.0
$\mathcal{B}(\bar{B}^0 \rightarrow D_1^+ \ell^- \bar{\nu}_\ell) \times 10^3$	6.40 ± 0.44	6.2 ± 0.5	6.24 ± 0.54
$\mathcal{B}(\bar{B}^0 \rightarrow D_0(2300)^+ \pi^-) \times 10^4$	1.19 ± 0.12	Not used	1.14 ± 0.12
$\mathcal{B}(\bar{B}^0 \rightarrow D_0(2300)^+ \ell^- \bar{\nu}_\ell) \times 10^3$	2.2 ± 1.2	4.1 ± 0.7	3.9 ± 0.7^d
$\mathcal{B}(\bar{B}^0 \rightarrow D_1(2430)^+ \pi^-) \times 10^4$	0.21 ± 0.27^a	Not used	Not quoted
$\mathcal{B}(\bar{B}^0 \rightarrow D_1(2430)^+ \ell^- \bar{\nu}_\ell) \times 10^3$	1.4 ± 1.3	1.9 ± 0.5	1.8 ± 1.5^d
$\mathcal{B}(\bar{B}^0 \rightarrow D_0(2300)^+ K^-) / \mathcal{B}(\bar{B}^0 \rightarrow D_2^{*+} K^-)^b$	0.84 ± 0.36	Not used	

^aWe have not used the measured value for $\mathcal{B}(\bar{B}^0 \rightarrow D_1(2430)^+ \pi^-)$ [28] as a constraint in our nominal fit because this is still a preliminary result; we have instead compared this value to our expectation.

^b $D^{**,+}$ mesons are reconstructed in the $D^0 \pi^+$ final state.

^cValues from PDG and HFLAV have been modified using results quoted in Table VI.

^dValues are from HFLAV [6], and the uncertainty on $\mathcal{B}(\bar{B}^0 \rightarrow D_1(2430)^+ \ell^- \bar{\nu}_\ell)$ is multiplied by a factor of 3 to account for the poor compatibility between the three measurements used to obtain the average value.

In addition, the Belle Collaboration [8] has measured the semileptonic decay branching fraction $\bar{B}^0 \rightarrow D_2^{*+} \ell^- \bar{\nu}_\ell$ in four bins of the variable $w = v_D \cdot v_B = (m_B^2 + m_{D_2^*}^2 - q^2) / 2m_B m_{D_2^*}$; $q^2 = m^2(\ell^- \bar{\nu}_\ell)$ (see Table V). The sum of these fractions is normalized to unity; therefore, in the following, because we do not have the full error matrix on these measurements available, we use the first three results and assume that they are independent.

Values quoted in the third column of Table IV are used in Appendix C to demonstrate that our code is able to reproduce the values obtained in [4] when using similar input values and hypotheses. Those given in the last column allow us to perform a comparison between experimental values retained in our analysis and those quoted in “official” compilations.

A. Evaluation of absolute $D^{**,+}$ decay branching fractions

At present, absolute D^{**} decay branching fractions are obtained using hypotheses on the contribution of the various decay channels. For the D_1 , it is assumed that it decays only into $D^* \pi$ and $D \pi \pi$ [through $D_0(2300) \pi$].

TABLE V. Measured fractions of the $\bar{B}^0 \rightarrow D_2^{*+} \ell^- \bar{\nu}_\ell$ decay width in several w bins.

w bin	Fraction (%)
[1.00, 1.08]	6.0 ± 2.3
[1.08, 1.16]	30.0 ± 5.4
[1.16, 1.24]	37.5 ± 6.2
[1.24, 1.32]	26.5 ± 6.2

The D_2^* is expected to decay only into $D \pi$ and $D^* \pi$. For broad states, we consider that the $D_0(2300)$ and the $D_1(2430)$ decay only into $D \pi$ and $D^* \pi$, respectively. Expected branching fractions are given in Table VI; they are similar to those used in [4].

B. Estimates for $\mathcal{B}(\bar{B}^0 \rightarrow D_{1/2}^+ \ell^- \bar{\nu}_\ell)$

Values for $D_0(2300)$ and $D_1(2430)$ production in \bar{B} hadron semileptonic decays, quoted in PDG or in HFLAV, are obtained by fitting expected $D^{(*)} \pi$ mass distributions on measured $\bar{B} \rightarrow D^{(*)} \pi \ell^- \bar{\nu}_\ell$ events. This approach is reliable for $D_{3/2}$ mesons which appear as relatively narrow mass peaks. The determination of broad $D_{1/2}$ production is more difficult because one also expects contributions from $D_V^{(*)} \rightarrow D^{(*)} \pi$, and it is not clear how these components have been included in the analyses. For these reasons we have adopted another approach.

To evaluate $\mathcal{B}(\bar{B}^0 \rightarrow D_{1/2}^+ \ell^- \bar{\nu}_\ell)$ we use $\mathcal{B}(\bar{B} \rightarrow D^{(*)} \pi \ell^- \bar{\nu}_\ell)$ exclusive measurements from BABAR [29] and Belle [30], from which we subtract the expected contributions from $D_{3/2}$ and $D_V^{(*)}$ decays.

TABLE VI. Expected absolute D^{**} meson decay branching fractions.

$\mathcal{B}(D_2^* \rightarrow D \pi)$	0.61 ± 0.02
$\mathcal{B}(D_1^+ \rightarrow D^{*0} \pi^+)$	0.45 ± 0.03
$\mathcal{B}(D_1^+ \rightarrow D^+ \pi^+ \pi^-)$	0.15 ± 0.02
$\mathcal{B}(D_1(2430) \rightarrow D^* \pi)$	1
$\mathcal{B}(D_0(2300) \rightarrow D \pi)$	1

It has to be noted that, at present, in all these evaluations, contributions from higher mass resonances, which can decay into $D^{(*)}\pi$, are not specifically evaluated and therefore are fully or partially included in the rates estimated for $D_{1/2}$ mesons, depending on the approach.

The $D_V^{(*)}$ components are normalized in an absolute way using values for $\mathcal{B}(\bar{B}^0 \rightarrow D^{(*)+}\ell^-\bar{\nu}_\ell)$ in which $D^{(*)}$ are on-mass shell, albeit with rather large uncertainties related to their mass dependence [2].

In the $D\pi$ channel, only the D_V^* component contributes. It is expected to decrease with the $D\pi$ mass value. For the D_V^{*0} channel, there is a natural threshold in the decay to $D^+\pi^-$ because $m_{D^{*0}} < m_{D^+} + m_{\pi^-}$. For other charge combinations, the separation between so-called D^* and D_V^* components is arbitrary, and therefore, the absolute value of the D_V^* component depends on the considered threshold. Belle uses the following mass range $m_{D^{(*)}\pi} \in [2.05, 3]$ GeV/ c^2 whereas BABAR requires $m_{D^{*0}\pi^+} - m_{D^0} > 0.18$ GeV/ c^2 . These cuts are rather similar, being typically 40 MeV/ c^2 above the nominal D^* mass.

To evaluate the uncertainty on these estimates, we assume that the $D_V^{(*)}$ follows a relativistic Breit-Wigner mass distribution, modified by a Blatt-Weisskopf damping term with the parameter $r_{\text{BW}} = 1.85$ (GeV/ c) $^{-1}$, which is varied in the range [1.0, 3.0] (GeV/ c) $^{-1}$.

1. $\mathcal{B}(\bar{B}^0 \rightarrow D_0(2300)^+\ell^-\bar{\nu}_\ell)$

Averaging experimental measurements one obtains $\mathcal{B}(\bar{B}^0 \rightarrow D\pi\ell^-\bar{\nu}_\ell) = (6.14 \pm 0.53) \times 10^{-3}$. We estimate the $D_V^* \rightarrow D\pi$ contribution, with $m_{D\pi} > 2.05$ GeV, to be equal to $(2.0 \pm 0.6) \times 10^{-3}$, in which the uncertainty corresponds to the variation range used for r_{BW} . The D_2^* contribution is obtained from Tables IV and VI; it amounts to $(1.90 \pm 0.18) \times 10^{-3}$.

This gives

$$\mathcal{B}(\bar{B}^0 \rightarrow D_0(2300)^+\ell^-\bar{\nu}_\ell) = (2.2 \pm 1.2) \times 10^{-3} \quad (12)$$

as reported, after rounding, in Table IV. The uncertainty on the D_V^* estimate is added linearly to the total uncertainty evaluated for the other sources.

2. $\mathcal{B}(\bar{B}^0 \rightarrow D_1(2430)^+\ell^-\bar{\nu}_\ell)$

We use the same approach for the $D^*\pi$ hadronic final state. Averaging experimental measurements, one obtains $\mathcal{B}(\bar{B}^0 \rightarrow D^*\pi\ell^-\bar{\nu}_\ell) = (8.39 \pm 0.54) \times 10^{-3}$. We estimate the D_V^{*+} contribution, using the coupling $g_{D^*D\pi} = \sqrt{2\frac{m_{D^*}}{m_D}}g_{D^*D\pi}$, which corresponds to a fictitious $\Gamma(D^* \rightarrow D^*\pi) = 2\Gamma(D^* \rightarrow D\pi)$, and we have added the expected (small) contribution from $D_V \rightarrow D^*\pi$. This gives $(1.4 \pm 0.6) \times 10^{-3}$. The D_V and D_V^* contributions are added incoherently because of helicity conservation and

the vanishing of $A - V$ interferences for the zero helicity after the angular integration.

Subtracting the D_1^+ $((4.32 \pm 0.41) \times 10^{-3})$ and D_2^{*+} $((1.21 \pm 0.14) \times 10^{-3})$ contributions, obtained from Tables IV and VI, gives

$$\mathcal{B}(\bar{B}^0 \rightarrow D_1(2430)^+\ell^-\bar{\nu}_\ell) = (1.4 \pm 1.3) \times 10^{-3} \quad (13)$$

as reported in Table IV. The uncertainty on the $D_V^{(*)}$ estimate is added linearly.

IV. PARAMETRIZATION OF SEMILEPTONIC AND NONLEPTONIC DECAY WIDTHS

We indicate here the expressions we use to compute semileptonic and nonleptonic class I decay branching fractions and explain how we have taken into account effects from contributions of virtual states.

A. Semileptonic transitions to real, discrete charmed states

Differential semileptonic $\bar{B} \rightarrow D_X\ell^-\bar{\nu}_\ell$ decay widths, with $D_X = D^{(**)}$, can be written as [4]

$$\frac{d\Gamma}{dq^2} = C|\vec{p}|q^2 \left(1 - \frac{m_\ell^2}{q^2}\right)^2 \times \left[(H_+^2 + H_-^2 + H_0^2) \left(1 + \frac{m_\ell^2}{q^2}\right) + \frac{3m_\ell^2}{2q^2} H_T^2 \right] \quad (14)$$

with $C = G_F^2 |V_{cb}|^2 \eta_{\text{EW}}^2 / (96\pi^3 m_B^2)$. Here, \vec{p} is the magnitude of the three-momentum of the D_X in the B rest frame,

$$|\vec{p}| = m_{D_X} \sqrt{w_{D_X}^2 - 1}, \quad (15)$$

in which $w_{D_X} = v_B \cdot v_{D_X}$ is the product of the 4-velocities of the two mesons.

Note that $H_{\pm,0,t}$ are helicity form factors which are expressed in terms of q^2 dependent, Lorentz invariant form factors $[FF(q^2)]$ and depend on the considered meson D_X . Accurate parametrizations of $FF(q^2)$ are obtained for D (we use [31]) and D^* mesons (we use [32,33]). For D^{**} mesons, expressions are taken from [3]. They correspond to expansions at first order in $1/m_{c,b}$ and α_s . For $D_{3/2}$ mesons, expressions that contain $1/m_{c,b} \times \alpha_s$ corrections are also available and have been included.

B. Semileptonic transitions to virtual charmed states

Let us now consider the physical case where the charmed state terminates on a two-body continuum like $D^{(*)}\pi$. As a useful intermediate step, one now considers fictitious weak transitions to intermediate virtual D^{**} or $D^{(*)}$, which represent the weak vertex part of the overall process, with the charmed leg bearing a momentum squared

$p^2 = m^2 (= m_{D^{(*)}\pi}^2)$, different from the nominal squared mass of the state $m_{D_X}^2$ (of course, in the overall process, leading, for instance, to a $D\pi$ final state, one has to introduce a D^* propagator relating the weak vertex to the strong vertex which couples the virtual state to $D\pi$). If one considers production of virtual D^{**} mesons (which will get a Breit-Wigner distribution for m) or of virtual $D^{(*)}$ (denoted usually as $D_V^{(*)}$) mesons, with m higher than their nominal mass value $m_{D^{(*)}}$, the invariant form factors at the weak vertex are expected to also be dependent on $m \neq m_{D_X}$.

However, in the absence of theoretical knowledge of this dependence, we assume simply

$$FF(m, q^2) = FF(m_{D_X}, q^2) \quad (16)$$

in the expressions of helicity form factors, while keeping $m \neq m_{D_X}$ dependence of the kinetic quantities, such as momenta, in the additional factors entering in these expressions. This procedure is illustrated in the following example of the production of a virtual D_V meson of mass $m \neq m_D$. There are two invariant form factors noted: $f_{+,0}(m, q^2)$. Helicity form factors are expressed as

$$\begin{aligned} qH_0 &= 2m_B |\vec{p}| f_+(m_D, q^2) \\ qH_t &= (m_B^2 - m^2) f_0(m_D, q^2). \end{aligned} \quad (17)$$

The two other form factors, H_{\pm} , vanish because of helicity conservation. In these expressions and in Eq. (14), the decay momentum is evaluated at the virtual mass m : $|\vec{p}| = m\sqrt{w^2 - 1}$ with $w = (m_B^2 + m^2 - q^2)/(2mm_B)$. Expressions relating helicity and invariant form factors when a D^* meson is emitted can be found in [33] and in [4] in the case of D^{**} mesons. Since these formulas are devised for real, discrete charmed states, one must modify the factors affecting the form factors when considering virtual charmed states.

C. Nonleptonic decays

Thanks to factorization, nonleptonic class I decay widths $\Gamma(\bar{B}^0 \rightarrow D_X^+ P^-)$ are related to the corresponding differential semileptonic decay widths, through the $H_t^{D_X}$ helicity form factor:

$$\begin{aligned} \Gamma(\bar{B}^0 \rightarrow D_X^+ P^-) \\ = \frac{|a_{1,\text{eff}}^{D_X\pi}|^2 f_P^2 G_F^2 |V_{ij}|^2 |V_{cb}|^2 |\vec{p}|}{16\pi m_B^2} q^2 (H_t^{D_X})^2|_{w_P}. \end{aligned} \quad (18)$$

In this expression, $q^2 = m_P^2$, f_P is the leptonic decay constant of the emitted charged meson P , and V_{ij} is the corresponding CKM matrix element,

$$w_P = \frac{m_B^2 + m_{D_X}^2 - m_P^2}{2m_B m_{D_X}}. \quad (19)$$

If the virtual ‘‘mass’’ m of the D_X meson does not have the nominal value m_{D_X} , we will still use values of invariant form factors evaluated at $q^2 = m_P^2$ as above while taking the running mass to compute the other terms that enter in $H_t^{D_X}$ and in \vec{p} .

We call the factor $a_{1,\text{eff}}^{D_X\pi}$ ‘‘effective’’ because the nonleptonic decay width, which enters in Eq. (18), corresponds to the sum of the class I diagram amplitude and of subdominant terms which correspond to exchange or penguin mechanisms, while the remaining factors in the right-hand side are those provided by the analytic expression for a pure class I process.

Expressions for $\bar{B}^0 \rightarrow D^{**,+} P^-$ partial decay widths, with $P = \pi^-$ or D_s^- , are given in Appendix A. Corresponding quantities, obtained in the infinite quark mass limit, for nonleptonic— $\Gamma(\bar{B}^0 \rightarrow D^{**}\pi^-)$ —and for the differential semileptonic— $d\Gamma(\bar{B}^0 \rightarrow D^{**,+} \ell^- \bar{\nu}_\ell)/dw$ —can be found, for example, in [34].

D. Finite width effects

To include effects from the mass distribution of resonances, we express the differential decay width for a process in which a D^{**} is reconstructed in a given final state (i) as [2]

$$\frac{d\Gamma_i}{ds} = \frac{1}{\pi} \frac{\Gamma_0(s) \sqrt{s} \Gamma_{i,D^{**}}(s)}{(s - m_{D^{**}}^2)^2 + s \Gamma_{D^{**}}^2(s)}. \quad (20)$$

Here, $\Gamma_0(s)$ is the decay width for the process computed in the hypothesis of a virtual D^{**} of mass equal to \sqrt{s} , and $\Gamma_{i,D^{**}}(s)$ is the partial decay width for the D^{**} , of mass \sqrt{s} , reconstructed in the i observed channel. Finally, $\Gamma_{D^{**}}(s)$ is the total D^{**} decay width at the mass \sqrt{s} .

When the current mass (\sqrt{s}) is higher than the threshold for the i decay channel,

$$\Gamma_{i,D^{**}}(s) = \Gamma_{i,D^{**}}(m_{D^{**}}^2) \left(\frac{p_i}{p_i^0}\right)^{2L+1} \left(\frac{m_{D^{**}}}{\sqrt{s}}\right)^2 \left(\frac{F_{i,L}(p_i)}{F_{i,L}(p_i^0)}\right)^2. \quad (21)$$

Here, p_i and p_i^0 are the breakup momenta for the D^{**} decaying into the i channel at masses equal to \sqrt{s} and $m_{D^{**}}$, respectively, and $F_{i,L}(p_i)$ is a Blatt-Weisskopf damping factor. For decay channels with a threshold above the resonance mass, p_i^0 becomes imaginary and $F_{i,L}(p_i^0)$ cannot be evaluated. Under these conditions we take

$$\Gamma_{i,D^{**}}(s) = \frac{g_i^2}{24\pi} \frac{p_i^{2L+1}}{s} F_i^2(p_i) \quad (22)$$

in which g_i is the coupling of the D^{**} to the i channel. This expression is used, in the following, to evaluate contributions from virtual D or D^* mesons to $D^{(*)}\pi$ final states.

Note that $\Gamma_{D^{**}}(s)$ is the sum of all partial decay widths $\Gamma_{i,D^{**}}(s)$, into channels opened at the mass \sqrt{s} .

In nonleptonic decays, the expression in Eq. (20) is multiplied by another damping factor [denoted usually as $(F_{B,i}(p'_i)/F_{B,i}(p_i^0))^2$] to account for strong interaction effects due to the hadron emitted with the D^{**} . Here, p'_i is the momentum of the B decay products, evaluated in the B rest frame.⁸

V. CONSTRAINTS USED IN OUR ANALYSIS

The measurements used in our analysis are listed in Table IV, second column.

There are three theoretical constraints (see Table III):

- (1) The validity of the factorization is checked, using $D_{3/2}$ events (see Sec. VI); then, it is used as a constraint in the final fits with $a_{1,\text{eff}}^{D^{**}\pi} = 0.93 \pm 0.07$ for all D^{**} states.
- (2) At $w = 1$ we use the constraint $\tau_{3/2}(1) = 0.53 \pm 0.03$ as expected from LQCD [9]. Because $\tau_{3/2}$ is defined in the infinite quark mass limit, it is necessary to introduce mass corrections and one parameter characterizing them, $\hat{\epsilon}_{3/2}$, [see Eq. (12)], which is a useful combination of the basic ones introduced by LLSW. Note that $\hat{\epsilon}_{3/2}$ is fitted, as well as part of the other parameters. The data on $D_{1/2}$ mesons are less accurate, and it is not possible to fit $\hat{\epsilon}_{1/2}$.
- (3) At $w \neq 1$, LQCD does not provide any information on the variation with respect to w of the two IW functions for which we use quark models, namely, the BT calculations explained in the second section. Unfortunately, quark models cannot provide errors. Therefore, to use them in a fit, we have considered a rather large range of values of the slopes around the predicted one.

A. Comparison with the analysis of [5]

To validate our code, we check that, using the same input data (given in the third column of Table IV) and the same hypotheses, we reproduce the results published in [5] (see Appendix C).

VI. PRODUCTION OF $D_{3/2}$ MESONS: A CHECK OF FACTORIZATION

In a first step, the analysis is restricted to the production of $D_{3/2}$ mesons to quantify the importance of $1/m_Q$ corrections and to check the applicability of the

factorization property. We require that $\tau_{3/2}(1) = 0.53 \pm 0.03$ and fit the $\hat{\epsilon}_{3/2}$ correction. This is essentially equivalent to directly fitting $\tau_{3/2}^{\text{eff}}$. No constraint is used on $a_{1,\text{eff}}^{D_{3/2}\pi}$ and $\sigma_{3/2}^2$.

Data are first analyzed without any $1/m_Q$ correction. The fit probability is below 10^{-13} . This is mainly due to the fact that, in the infinite quark mass limit, theory predicts a production higher for the D_2^* as compared to the D_1 whereas it is measured to be 2 times lower.

Adding set 1 of $1/m_Q$ corrections improves the situation, but the fit probability is still below 10^{-4} .

Therefore, it is necessary to fit additional parameters which control the other $1/m_Q$ corrections. Successively fitting one among all other parameters, we end up with the results given in Table VII. All fit probabilities are higher than 10%.

It can be noted that, depending on the choice of the additional fitted parameter, values of the slope ($\sigma_{3/2}^2$) and of the correction ($\hat{\epsilon}_{3/2}$) to the normalization of the IW function fluctuate. This comes from the fact that fitted individual parameters are also changing the w dependence of form factors, and there are not enough measurements of the differential decay branching fractions versus w to constrain these variations. Thus, fitted values for the IW slope can be highly correlated with the value fitted for some of the additional parameters. In the following we therefore use the constraint expected from QM: $\sigma_{3/2}^2 = 1.5 \pm 0.5$; thus, the w dependence of the IW function verifies expectations from theory, while we have no constraints on the precise values of all parameters entering in $1/m_Q$ corrections. One has to check, *a posteriori*, that such quantities are not too large so that the model we are using remains valid.

Results obtained for all possible fitted pairs of parameters are given in Table VIII. The fitted correction $\hat{\epsilon}_{3/2}$ is now rather independent on the choice of the fitted pair.

The value of $a_{1,\text{eff}}^{D_{3/2}\pi}$, fitted in each model (see Tables VII and VIII), varies between 0.81 and 1.06 with uncertainties between 0.05 and 0.11. This is compatible with estimates of $a_{1,\text{eff}}^{D\pi} = 0.880 \pm 0.024$ and $a_{1,\text{eff}}^{D^*\pi} = 0.981 \pm 0.025$ that we obtain by analyzing corresponding decay channels. These values differ somewhat from the one given by BBNS, but this is not unexpected since we are far from the asymptotic situation considered by those authors.

Therefore, in our final results we add, as a constraint, that $a_{1,\text{eff}}^{D^{**}\pi} = 0.93 \pm 0.07$, obtained from the measurements when either a D or a D^* is produced. This constraint is important, when evaluating systematic uncertainties, to avoid effects of a variation of a given parameter inducing a large variation on a_1 and therefore corresponding to effects that are outside the fact that the present analysis is done in the framework of factorization. This constraint is softer than the one used for this same property in previous analyses of these channels.

⁸In some analyses, p' is evaluated in the resonance rest frame. We consider that our choice is more physical. Effects of changing the convention to compute p' are given in Table XIII.

TABLE VII. Results obtained using the constraint from theory on $\tau_{3/2}(1)$. Set 1 $1/m_Q$ corrections are used, and one additional parameter from set 2 is fitted, in addition to $\hat{\epsilon}_{3/2}$.

X param.	$a_{1,\text{eff}}^{D_{3/2}\pi}$	$\sigma_{3/2}^2$	$\hat{\epsilon}_{3/2}$	X (GeV)	χ^2/NDF
$\hat{\eta}_1$	0.90 ± 0.05	-0.4 ± 0.7	-0.50 ± 0.09	-0.40 ± 0.11	3.4/4
$\hat{\eta}_3$	0.82 ± 0.05	-2.1 ± 0.7	-0.77 ± 0.07	3.2 ± 1.1	7.0/4
$\hat{\tau}_1$	0.81 ± 0.07	1.0 ± 0.7	-0.34 ± 0.12	0.75 ± 0.24	6.4/4
$\hat{\tau}_2$	0.89 ± 0.06	2.1 ± 0.5	-0.19 ± 0.11	2.9 ± 0.8	2.5/4
$\hat{\eta}_2$	0.86 ± 0.06	1.2 ± 0.6	-0.30 ± 0.11	-1.63 ± 0.44	3.8/4

A. Fitted model parameters for $D_{3/2}$ production

As observed in Tables VII and VIII, the χ^2 obtained when fitting present data is mainly sensitive to the parameters $\hat{\eta}_1$, $\hat{\eta}_3$, and $\hat{\tau}_1$. There are enough measurements and constraints to determine these quantities with some accuracy. Values of the two other parameters, $\hat{\tau}_2$ and $\hat{\eta}_2$, cannot be determined from present data. We have evaluated effects from this indetermination by changing the values of these two quantities by ± 0.5 GeV and by redoing the fit of the other parameters. The variation range we consider is obtained by noting that these quantities can have, at most, values similar to $\bar{\Lambda}$ so that the model remains valid.

B. Summary on $D_{3/2}$ production

In summary, production of $D_{3/2}$ in nonleptonic class I B -meson decays is compatible with factorization.

The analysis can be done using the value expected from LQCD for $\tau_{3/2}(1) = 0.53 \pm 0.03$, but this differs from the $\tau_{3/2}^{\text{eff}}(1)$ introduced in Eq. (11) by the quantity $\hat{\epsilon}_{3/2} = -0.2 \pm 0.1$, whose value has been fitted. We have verified, in Appendix B, that the minus sign of this correction agrees with theory. Combining these values we obtain

$$\tau_{3/2}^{\text{eff}}(1) = 0.42 \pm 0.06, \quad (23)$$

in agreement with previous analyses.

To have reasonable agreement between data and expectations, we find that it is necessary to fit at least one among the five parameters that control $1/m_Q$ corrections. In this case there remain four parameters that are unknown, and it is difficult to obtain model uncertainties. Hopefully, present measurements and constraints from theory will allow us to evaluate values of the three most important parameters that control the model. In this way we estimate that we have better control of systematic uncertainties that come from estimates of the values of quantities that are not fitted on data. We obtain

$$\begin{aligned} \hat{\eta}_1(\text{GeV}) &= -0.32 \pm 0.13 \pm 0.03 \\ \hat{\eta}_3(\text{GeV}) &= -0.77 \pm 0.28 \pm 0.21 \\ \hat{\tau}_1(\text{GeV}) &= 0.36 \pm 0.35 \pm 0.35, \end{aligned} \quad (24)$$

in which the second uncertainty corresponds to the largest variations induced by changing the values of $\hat{\tau}_2$ and $\hat{\eta}_2$ by ± 0.5 GeV. We consider that this model uncertainty has to be added linearly to the one coming from the fit because we cannot favor any value for $\hat{\tau}_2$ and $\hat{\eta}_2$, within their considered variation range.

One cannot directly compare values obtained for $\hat{\eta}_{1,3}$ and $\hat{\tau}_1$ with previous determinations in which one or at most two of these parameters have been fitted on data. It can be noted that fitted values do not preclude the assumed validity of the $1/m_Q$ expansion because these quantities are of order $\bar{\Lambda}$. In Table IX we compare expected values for the ratios

TABLE VIII. Results obtained using the two constraints from theory on $\tau_{3/2}(1)$ and $\sigma_{3/2}^2$. Set 1 $1/m_Q$ corrections are used, and two additional parameters from set 2 are fitted, in addition to $\hat{\epsilon}_{3/2}$.

$X - Y$ param.	$a_{1,\text{eff}}^{D_{3/2}\pi}$	$\sigma_{3/2}^2$	$\hat{\epsilon}_{3/2}$	X (GeV)	Y (GeV)	χ^2/NDF
$\hat{\eta}_1 - \hat{\eta}_3$	1.06 ± 0.08	1.45 ± 0.45	-0.19 ± 0.11	-0.45 ± 0.08	-0.78 ± 0.25	1.4/4
$\hat{\eta}_1 - \hat{\tau}_1$	0.83 ± 0.11	1.34 ± 0.57	-0.28 ± 0.10	0.05 ± 0.26	0.68 ± 0.73	6.7/4
$\hat{\eta}_1 - \hat{\tau}_2$	0.88 ± 0.06	1.55 ± 0.50	-0.27 ± 0.09	-0.07 ± 0.10	2.34 ± 1.24	2.7/4
$\hat{\eta}_1 - \hat{\eta}_2$	0.86 ± 0.06	1.55 ± 0.50	-0.24 ± 0.10	0.09 ± 0.17	-2.1 ± 1.1	3.7/4
$\hat{\eta}_3 - \hat{\tau}_1$	0.82 ± 0.05	1.75 ± 0.50	-0.18 ± 0.12	-0.52 ± 0.33	1.04 ± 0.31	4.6/4
$\hat{\eta}_3 - \hat{\tau}_2$	0.86 ± 0.05	1.66 ± 0.50	-0.27 ± 0.11	0.10 ± 0.23	2.9 ± 0.9	3.0/4
$\hat{\eta}_3 - \hat{\eta}_2$	0.89 ± 0.05	1.67 ± 0.48	-0.19 ± 0.11	-0.30 ± 0.26	-2.0 ± 0.5	2.8/4
$\hat{\tau}_1 - \hat{\tau}_2$	0.86 ± 0.06	1.75 ± 0.46	-0.25 ± 0.09	0.07 ± 0.33	2.8 ± 1.5	3.2/4
$\hat{\tau}_1 - \hat{\eta}_2$	0.98 ± 0.10	1.60 ± 0.41	-0.20 ± 0.10	-1.1 ± 0.7	-3.9 ± 1.6	1.9/4
$\hat{\tau}_2 - \hat{\eta}_2$	0.87 ± 0.05	1.65 ± 0.48	-0.25 ± 0.09	2.1 ± 2.2	-0.5 ± 1.1	3.0/4

TABLE IX. Comparison between expected values for $\mathcal{R}_{D_{3/2}}$.

$\mathcal{R}_{D_{3/2}}(\%)$	Our analysis	Reference [4] (2016)	Reference [5] (2017)
$\mathcal{R}_{D_2^*}$	$6.1 \pm 0.5 \pm 0.2$	7 ± 1	7 ± 1
\mathcal{R}_{D_1}	$9.9 \pm 0.7 \pm 0.1$	10 ± 1	10 ± 2

$\mathcal{R}_{D_{3/2}} = \mathcal{B}(\bar{B}^0 \rightarrow D_{3/2}^+ \tau^- \bar{\nu}_\tau) / \mathcal{B}(\bar{B}^0 \rightarrow D_{3/2}^+ \ell^- \bar{\nu}_\ell)$ with previous determinations.

VII. PRODUCTION OF $D_{1/2}$ MESONS:

$$\tau_{1/2}^{\text{eff}}(\mathbf{1}) \ll \tau_{3/2}^{\text{eff}}(\mathbf{1})$$

Data on B -meson semileptonic decays into $D_{1/2}$ states are rather uncertain. In agreement with previous analyses (see Table XVII in Appendix C), we find that present data do not allow us to determine the slope $\sigma_{1/2}^2$ of the corresponding IW function. In addition, the effect of $1/m_Q$ parameters is to modify the observed w dependence of form factors; therefore, it is important, as explained in the previous section, to ensure that the variation of the IW function remains physical. Following relativistic quark model expectations, we use $\sigma_{1/2}^2 = 0.8$ with a conventional error ± 0.5 .

For the same reasons, it is not possible to fit the parameter $\hat{e}_{1/2}$.

Using measurements, relative to $D_{1/2}$ production in Table IV, apart from $\mathcal{B}(\bar{B}^0 \rightarrow D_1(2430)^+ \pi^-)$, which is not published, and factorization with $a_1 = 1$, we have fitted $\tau_{1/2}^{\text{eff}}(\mathbf{1})$ (see Table X).

Without fitting any additional $1/m_Q$ parameter, we obtain

$$\tau_{1/2}^{\text{eff}}(\mathbf{1}) = 0.147 \pm 0.025, \quad (25)$$

with a 24% fit probability. This value is much smaller than $\tau_{3/2}^{\text{eff}}(\mathbf{1})$ given in Eq. (23), in agreement with the theoretical expectations and in contradiction with LLSWB.

Let us now take into account the $1/m_Q$ corrections. The $\hat{\chi}_{1,2}$ and $\hat{\zeta}_1$ correction parameters provide enough flexibility in decay rate expressions to accommodate essentially any measured values, with an acceptable χ^2 probability. It is therefore needed to use additional constraints from theory.

The LQCD expectation [9] gives $\tau_{1/2}(\mathbf{1}) = 0.296 \pm 0.026$. We have no predicted value for the quantity $\hat{e}_{1/2}$, which corresponds to $1/m_Q$ corrections on $\tau_{1/2}(\mathbf{1})$. If we assume that $\hat{e}_{1/2} = \hat{e}_{3/2}$, we expect $\tau_{1/2}^{\text{eff}}(\mathbf{1}) = 0.24 \pm 0.02$, which is higher than the measurement in Eq. (25). This can be due to either the fact that $\hat{e}_{1/2}$ differs from $\hat{e}_{3/2}$ or that other $1/m_Q$ corrections, not considered for the evaluation in Eq. (25), can have some effect. For these reasons, in the following, we use as a constraint the value

TABLE X. Fitted values of one of the parameters entering in $1/m_Q$ corrections. Note that $\tau_{1/2}^{\text{eff}}(\mathbf{1})$ and $\sigma_{1/2}^2$ are constrained as explained in the text.

X param.	$\tau_{1/2}^{\text{eff}}(\mathbf{1})$	$\sigma_{1/2}^2$	X	χ^2/NDF
no X	0.155 ± 0.025	1.0 ± 0.5	No value	3.5/3
χ_1	0.21 ± 0.06	0.80 ± 0.50	-0.27 ± 0.22	2.6/2
χ_2	0.21 ± 0.06	0.78 ± 0.50	0.37 ± 0.27	2.5/2
ζ_1	0.22 ± 0.06	0.76 ± 0.50	0.75 ± 0.44	2.3/2

$\tau_{1/2}^{\text{eff}}(\mathbf{1}) = 0.20 \pm 0.06$, where the uncertainty is large enough to cover the two previous estimates.

Using these two constraints [on $\tau_{1/2}^{\text{eff}}(\mathbf{1})$ and $\sigma_{1/2}^2$] and fitting one additional parameter, we obtain the values given in Table X.

Fit probabilities are close to 30%, and values for the different parameters are reasonable, of the order of $\bar{\Lambda}$. However, comparing with $D_{3/2}$ production, one cannot identify a parameter to which the analysis is most sensitive, and we are not able to fit more than one of these quantities, with reasonable accuracy, using present data. In the following we adjust $\hat{\chi}_1$ and evaluate model systematic uncertainties, changing $\hat{\chi}_2$ and $\hat{\zeta}_1$ by ± 0.5 GeV.

VIII. PRODUCTION OF $D_{3/2}$ AND $D_{1/2}$ MESONS: COMBINED ANALYSIS AND SYSTEMATIC UNCERTAINTIES

We include in the analysis the data given in Table IV, excluding the unpublished measurement of $\mathcal{B}(\bar{B}^0 \rightarrow D_1(2430)^+ \pi^-)$. Constraints from theory on the parameters of the IW functions and the list of fitted quantities are given in Table III, Sec. II D.

The analysis is done by taking into account the validity of factorization, for all D^{**} -meson production, and using $a_{1,\text{eff}}^{D^{**}\pi} = 0.93 \pm 0.07$; see Sec. VI.

The ratio $\chi^2/NDF = 6.3/7$ corresponds to a fit probability of 51%.

Values of fitted parameters, given in Table XI, are almost identical to those obtained when considering separate productions of $D_{3/2}$ and $D_{1/2}$ mesons (see Secs. VI B and VII).

Fitted quantities allow us to obtain values for different branching fractions of a \bar{B}^0 meson decaying into $D^{**} \ell^- \bar{\nu}_\ell$, with a light or τ lepton, as well as for nonleptonic decays.

We have also considered $\bar{B}^0 \rightarrow D^{**+} D_s^{(*)-}$ decays, in the framework of factorization.

To evaluate systematic uncertainties, values of unfitted parameters are changed to ± 0.5 GeV, and the largest variation on a fitted or derived quantity, which depends on fitted values, is used as the systematic model uncertainty. For some of these quantities, mainly related to the production of $D_{1/2}$ mesons, these variations are asymmetric, when compared to the value obtained with the reference

TABLE XI. Fitted values of the reference model parameters, for $B \rightarrow D^{**}$ Lorentz invariant form factors. The first line contains parameters that are constrained by theory or from external measurements ($a_{1,\text{eff}}^{D^{**}\pi}$). Quoted uncertainties are obtained from the fit.

$a_{1,\text{eff}}^{D^{**}\pi}$	$\tau_{3/2}(1)$	$\sigma_{3/2}^2$	$\tau_{1/2}^{\text{eff}}(1)$	$\sigma_{1/2}^2$
0.944 ± 0.062	0.53 ± 0.03	1.50 ± 0.50	0.21 ± 0.06	0.80 ± 0.70
$\hat{e}_{3/2}$	$\hat{\eta}_1$ (GeV)	$\hat{\eta}_3$ (GeV)	$\hat{\tau}_1$ (GeV)	$\hat{\lambda}_1$ (GeV)
-0.18 ± 0.11	-0.32 ± 0.13	-0.77 ± 0.28	0.36 ± 0.35	-0.24 ± 0.26

model (in which the non-fitted parameters are set to zero). In this case we have symmetrized systematic uncertainties and corrected central values accordingly. Model uncertainties are added linearly to those from the fit because there is no reason to prefer a value for unfitted quantities, within their variation range.

Other sources of systematic uncertainties are considered as follows:

- (i) Effects from uncertainties on HQET parameters (set 1). They are illustrated by using the values adopted in previous analyses (see Table II).
- (ii) Effects of using a linear parametrization for the IW functions, versus w , in place of the dipole distribution [Eq. (6)].
- (iii) Effect of changing the parametrization of Blatt-Weisskopf terms in nonleptonic decays when the momentum of the emitted hadron is computed in the frame of the resonance in place of the B -meson rest frame (the former has been used by some experimental collaborations).

These observed variations are only indicative and cannot be considered as really representative of corresponding systematic uncertainty values. In most cases, these sources are less important than uncertainties from the fit or from the model.

When evaluating a ratio between two derived quantities, correlations between the different uncertainties are taken into account.

In the following we detail our expectations and give comparisons with those obtained in another analysis, quoted as LLSWBi, which is close to those done in previous publications [4,5]. Differences relative to our approach are listed in Appendix D. Numerical values, obtained in this way, are quoted also in appendixes, whereas corresponding expected distributions are compared with our results on the different figures that follow.

A. Comparison between our model and the LLSWBi analysis for $D_{1/2}$ production in nonleptonic class I decays

In Table XII we illustrate the differences between our model and the LLSWBi analysis for class I nonleptonic decays.

The measured values for $\mathcal{B}(\bar{B}^0 \rightarrow D_0(2300)^+\pi^-)$ and $\mathcal{R}(D_0(2300), D_2^*)$ enter our model through the use of factorization. Therefore, it is a check of consistency that the corresponding fitted values are in agreement with the data, as well as with theory, which indeed predicts that $j = 1/2$ transitions should be much smaller than $j = 3/2$ ones.

On the other hand, one can see that predictions of LLSWBi are in disagreement with the data by more than 4 standard deviations and too large by around 1 order of magnitude, which leads us to discard the model. Keeping this in mind, it may nevertheless be useful to apply the same model to semileptonic decays for the sake of comparison with our own results, especially since LLSW is used by experimentalists in the analyses of the background to decays such as $\bar{B} \rightarrow D^* \ell \bar{\nu}_\ell$.

IX. D^{**} MESON PRODUCTION IN \bar{B}^0 SEMILEPTONIC DECAYS

Our results on decay branching fractions of \bar{B}^0 mesons into the four $D^{**,+}$ mesons are explained. In Secs. IX B and IX C, expected hadronic mass and q^2 distributions are obtained for the $D^*\pi$ and $D\pi$ hadronic final states, respectively. Spectra are compared with the LLSWBi analysis, and for ease of comparison, total decay rates, expected in the two cases, have been scaled (only for plotting purposes) to the central values measured for the considered final states. Corresponding uncertainties are also scaled to agree with those obtained on measurements

TABLE XII. Comparison between measured and expected values for nonleptonic $\bar{B}^0 \rightarrow D_{1/2}$ transitions. Here, $\mathcal{R}_K(D_0(2300), D_2^*)$ is the ratio between the branching fractions $\mathcal{B}(\bar{B}^0 \rightarrow D_0(2300)^+K^-)$ and $\mathcal{B}(\bar{B}^0 \rightarrow D_2^{*+}K^-)$, with the two D^{**} mesons decaying into $D^0\pi^+$.

Channel	Measured	Our model	LLSWBi model
$\mathcal{B}(\bar{B}^0 \rightarrow D_0(2300)^+\pi^-) \times 10^4$	1.19 ± 0.12	1.21 ± 0.12	10.0 ± 2.5
$\mathcal{B}(\bar{B}^0 \rightarrow D_1(2430)^+\pi^-) \times 10^4$	0.21 ± 0.27	0.7 ± 0.7	3.2 ± 2.8
$\mathcal{R}_K(D_0(2300), D_2^*)$	0.84 ± 0.36	0.35 ± 0.04	2.8 ± 0.7

for $\mathcal{B}(\bar{B}^0 \rightarrow D^{(*)+} \pi^- \ell^- \bar{\nu}_\ell)$, with light leptons. Additional uncertainties, from the fit and the model, which appear when considering decays with a τ lepton or a D_s^- meson, are included.

A. Expected values for $\mathcal{B}(\bar{B}^0 \rightarrow D_i^{*+,+} \ell^- \bar{\nu}_\ell)$ and corresponding q^2 distributions

Expected q^2 distributions in \bar{B}^0 semileptonic decays with a light or τ lepton are given in Figs. 1–4 for D_2^{*+} , D_1^+ , $D_0(2300)^+$, and $D_1(2430)^+$, respectively. Hatched areas correspond to uncertainties from the fit. Curves indicated

with dots are the expected systematic uncertainties from the unmeasured $\hat{\eta}_2$ and $\hat{\tau}_2$ parameters. Those indicated with triangles are from the unmeasured $\hat{\chi}_2$ and $\hat{\zeta}_1$ parameters. In each figure the left plot is for light leptons and the right one for the τ .

Expected values for semileptonic branching fractions, with a light and τ lepton, are given in Table XIII. Those obtained in the LLSWBi analysis are given in Appendix D 1. To evaluate uncertainties on quoted values, we have linearly added uncertainties from the fit and from the model. Values for other possible sources of uncertainties, quoted in Table XIII, are simply indicative and usually

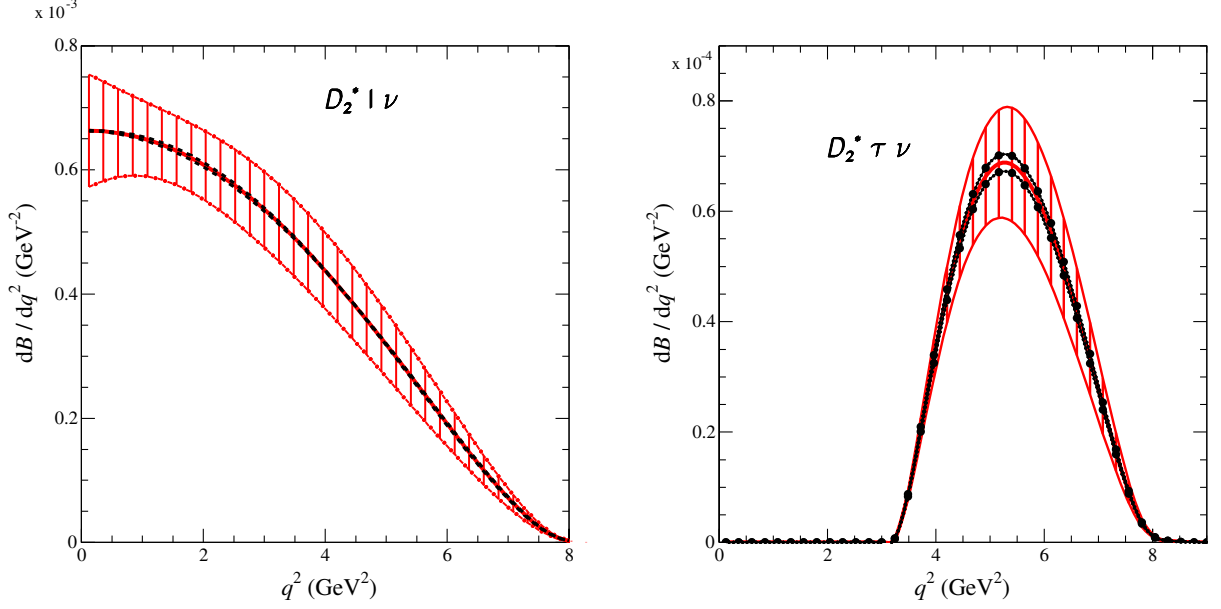


FIG. 1. Expected q^2 distributions for $\bar{B}^0 \rightarrow D_2^{*+}$ in semileptonic decays. Hatched areas correspond to uncertainties from the fit; curves with dots indicate the model uncertainty. Other systematic uncertainties, indicated in Table XIII, are not displayed.

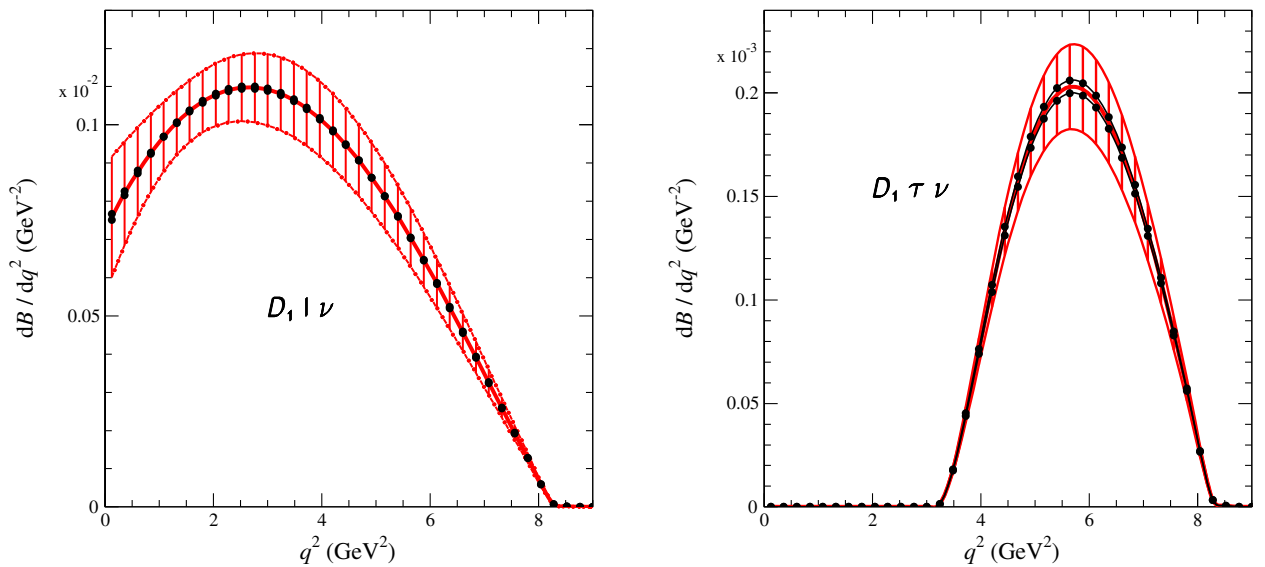


FIG. 2. Expected q^2 distributions for $\bar{B}^0 \rightarrow D_1^+$ in semileptonic decays. The same conventions are used as in Fig. 1.

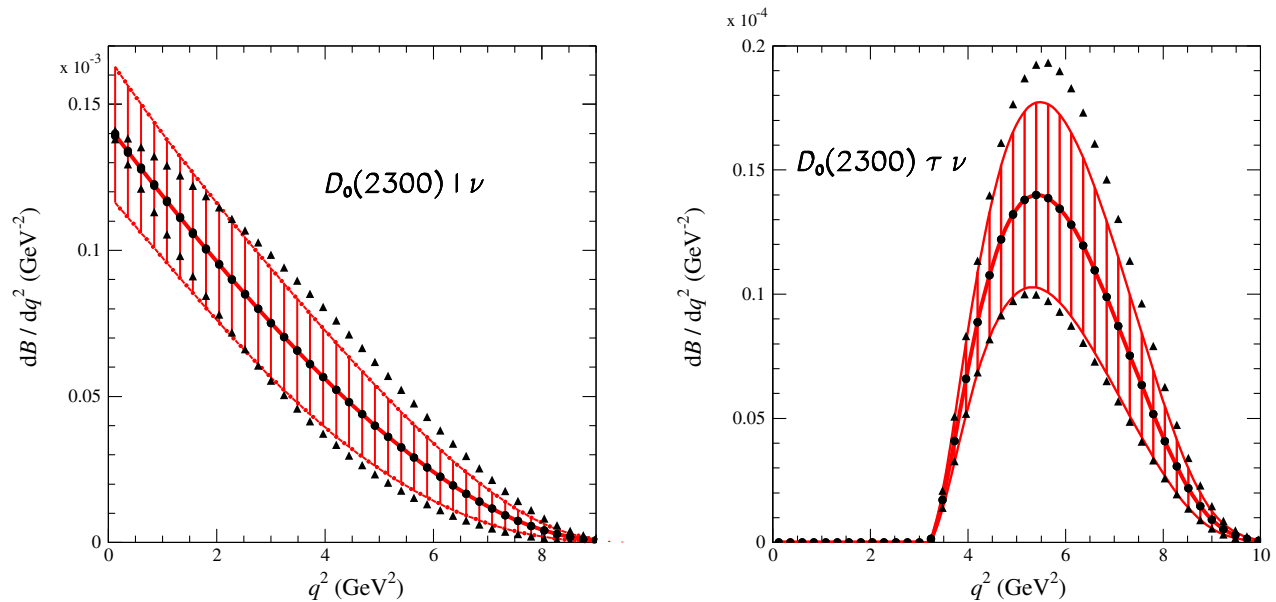


FIG. 3. Expected q^2 distributions for $\bar{B}^0 \rightarrow D_0(2300)^+$ in semileptonic decays. Hatched areas correspond to uncertainties from the fit; curves with dots indicate the model uncertainty expected from $\hat{\tau}_2$ and $\hat{\eta}_2$ parameters, whereas those with triangles correspond to the uncertainty from $\hat{\chi}_2$ and $\hat{\zeta}_1$. Other systematic uncertainties, given in Table XIII, are not displayed.

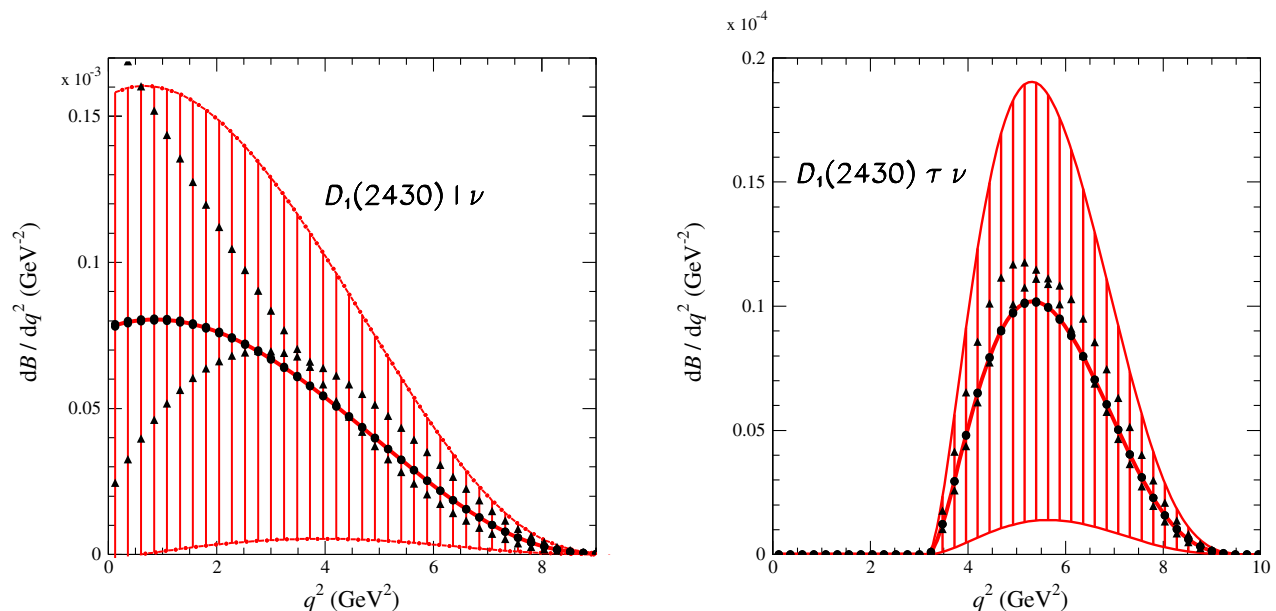


FIG. 4. Expected q^2 distributions for $\bar{B}^0 \rightarrow D_1(2430)^+$ in semileptonic decays. The same conventions are used as in Fig. 3.

are not dominant when compared with the others. It can be noted that ratios of branching fractions with a τ or a light lepton have a better accuracy because of correlations between the different uncertainties.

1. $D_{3/2}$ production

Values for semileptonic branching fractions with a light lepton and a $D_{3/2}$ meson are essentially identical to input

measurements. This is because one basically has no measurement of the q^2 dependence of the different decay rates and because the normalization is fitted through the $\tau_{3/2}$ and $\hat{\epsilon}_{3/2}$ parameters. Expected uncertainties on the production of D_1 and D_2^* , with a τ lepton are of about 20%. It can be noted that, in D_1 production, uncertainties on set 1 (HQET) parameters and on the w expected dependence of $\tau_{3/2}$ may not be negligible. This is expected because HQET

TABLE XIII. Our expectations for semileptonic branching fractions with a light or a τ lepton and their ratio for individual D^{**} -meson states.

Channel	Value \pm fit	Model	HQET	IW linear	Blatt-W.
$\mathcal{B}(\bar{B}^0 \rightarrow D_2^{*+} \ell^- \bar{\nu}_\ell) \times 10^3$	3.15 ± 0.30	0.00	0.00	0.01	0.02
$\mathcal{B}(\bar{B}^0 \rightarrow D_2^{*+} \tau^- \bar{\nu}_\tau) \times 10^4$	1.90 ± 0.29	0.05	0.00	0.09	0.03
$\mathcal{R}_{D_2^*} \times 10^2$	6.03 ± 0.52	0.15	0.02	0.24	0.06
$\mathcal{B}(\bar{B}^0 \rightarrow D_1^+ \ell^- \bar{\nu}_\ell) \times 10^3$	6.40 ± 0.44	0.00	0.00	0.00	0.00
$\mathcal{B}(\bar{B}^0 \rightarrow D_1^+ \tau^- \bar{\nu}_\tau) \times 10^4$	6.30 ± 0.59	0.10	0.30	0.70	0.07
$\mathcal{R}_{D_1} \times 10^2$	9.84 ± 0.68	0.15	0.47	1.10	0.11
$\mathcal{B}(\bar{B}^0 \rightarrow D_0(2300)^+ \ell^- \bar{\nu}_\ell) \times 10^4$	5.1 ± 1.2	1.2	-0.2	0.4	-0.1
$\mathcal{B}(\bar{B}^0 \rightarrow D_0(2300)^+ \tau^- \bar{\nu}_\tau) \times 10^5$	5.0 ± 1.3	1.7	-0.1	0.6	0.1
$\mathcal{R}_{D_0(2300)} \times 10^2$	9.9 ± 1.5	1.0	0.4	0.4	0.1
$\mathcal{B}(\bar{B}^0 \rightarrow D_1(2430)^+ \ell^- \bar{\nu}_\ell) \times 10^4$	4.6 ± 3.7	0.9	0.3	-0.5	0.0
$\mathcal{B}(\bar{B}^0 \rightarrow D_1(2430)^+ \tau^- \bar{\nu}_\tau) \times 10^5$	3.4 ± 2.7	0.6	0.3	-0.3	0.0
$\mathcal{R}_{D_1(2430)} \times 10^2$	7.4 ± 1.2	1.6	0.1	0.4	0.1

set 1 corrections change the computed branching fraction with a D_1 by a large factor, as compared with the infinite quark mass limit prediction.

2. $D_{1/2}$ production

The value expected for $\mathcal{B}(\bar{B}^0 \rightarrow D_0(2300)^+ \ell^- \bar{\nu}_\ell) = (5.1 \pm 2.4) \times 10^{-4}$ is much smaller than the one usually anticipated from LLSWBi: $(39.1 \pm 7.2) \times 10^{-4}$, as given in Appendix D 1. This result is a direct consequence of the use of factorization. Values expected for $D_1(2430)$ are similar, but being affected by larger uncertainties, one cannot draw any conclusions. Production of $D_{1/2}$ mesons in B -meson semileptonic decays is expected to be an order of magnitude smaller than the one of narrow states. In the production of $D_{1/2}$ mesons, model uncertainties are dominant when compared with the other considered sources of systematic uncertainties.

Expected branching fractions for $D_0(2300)$ and $D_1(2430)$ production have about 50% and 100% uncertainty, respectively. These relative uncertainties are even larger when a τ lepton is emitted.

3. Conclusions

In our analysis, the expected low production rates of broad, relative to narrow, D^{**} mesons come from theoretical arguments and are in agreement with the factorization property. This low value implies that it has to be complemented by another source of events, to explain the measured broad mass distributions in $D^{(*)}\pi$ hadronic final states. We examine, in the following sections, if the contributions expected from $D_V^{(*)}$ components can fill these gaps. Such components have been ignored in previous analyses which consider that $D_{1/2}$ decays, alone, are enough to explain measurements.

B. Analysis and predictions for the $\bar{B}^0 \rightarrow D^* \pi \ell^- \bar{\nu}_\ell$ final state

We examine if measured $\bar{B}^0 \rightarrow D^* \pi \ell^- \bar{\nu}_\ell$ decays can be explained using a sum of D^{**} and $D_V^{(*)}$ components. All quoted numbers are relative to the sum of $D^{*0}\pi^+$ and $D^{*+}\pi^0$ final states, and we refer to Sec. III B 2 for input measurements.

The measured branching fraction into broad components amounts to

$$\mathcal{B}(\bar{B}^0 \rightarrow D^* \pi|_{\text{broad}} \ell^- \bar{\nu}_\ell) = (2.86 \pm 0.69) \times 10^{-3}. \quad (26)$$

In the hypothesis that contributions from higher mass resonances can be neglected, the expected contribution from $D_1(2430)^+$ decays, equal to $(0.46 \pm 0.46) \times 10^{-3}$, has to be complemented by a $D_V^{(*)}$ component equal to $(2.4 \pm 0.8) \times 10^{-3}$. For r_{BW} values varying between 1 and 3 GeV^{-1} , our estimates for this component are in the range $[2.0, 0.9] \times 10^{-3}$ (see Sec. III B 2). These values are compatible with the needed contribution.

In Fig. 5, expected $D^* \pi$ mass distributions from our model (solid line) and from the LLSWBi analysis (dashed line) are compared. To ease the comparison, central values expected from the two models are scaled to agree with the measured one. To do so, in our model, only the $D_V^{(*)}$ component is scaled, while, for other components, the expected values are used. In LLSWBi, only the $D_1(2430)^+$ component is scaled. Scaling factors are obtained for decays into light leptons, and their values are used for the other analyzed transitions which involve a τ lepton or a D_s meson.

Spectra are dominated by the contributions from $D_{3/2}$ mesons.

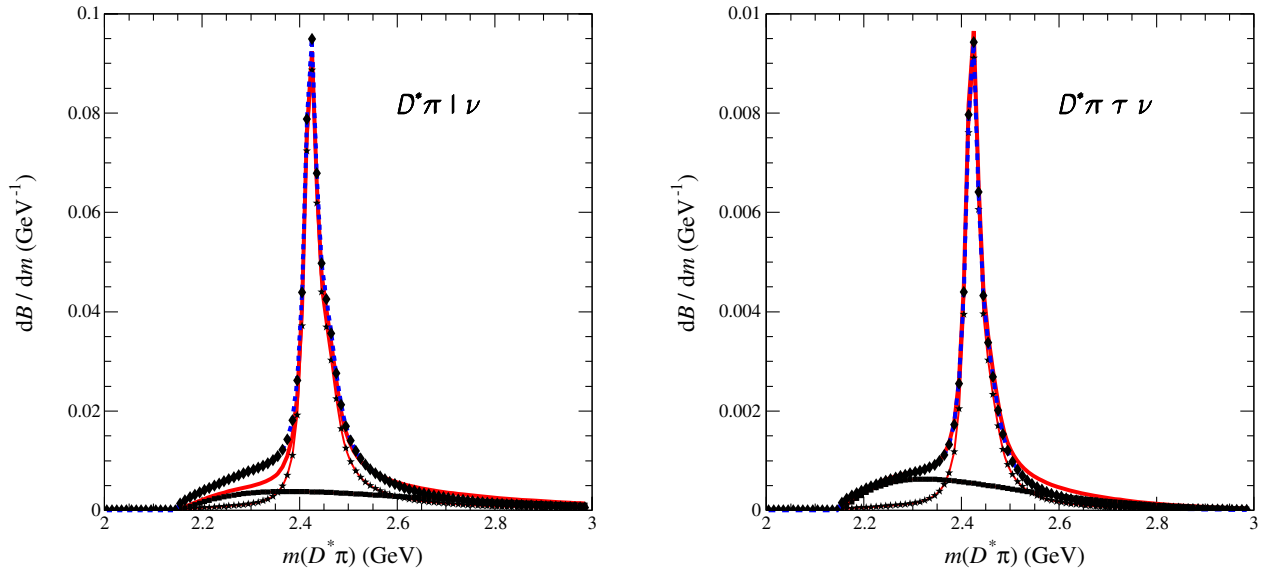


FIG. 5. Expected $D^*\pi$ mass distributions for $\bar{B}^0 \rightarrow D^*\pi$ in semileptonic decays. Solid lines correspond to our model, and the dashed line is for LLSWBi. The line with stars gives the D^{**} contribution, and the one with squares is for the $D_V^{(*)}$ component. The red line corresponds to the sum of these two contributions. Only central values of the distributions are displayed.

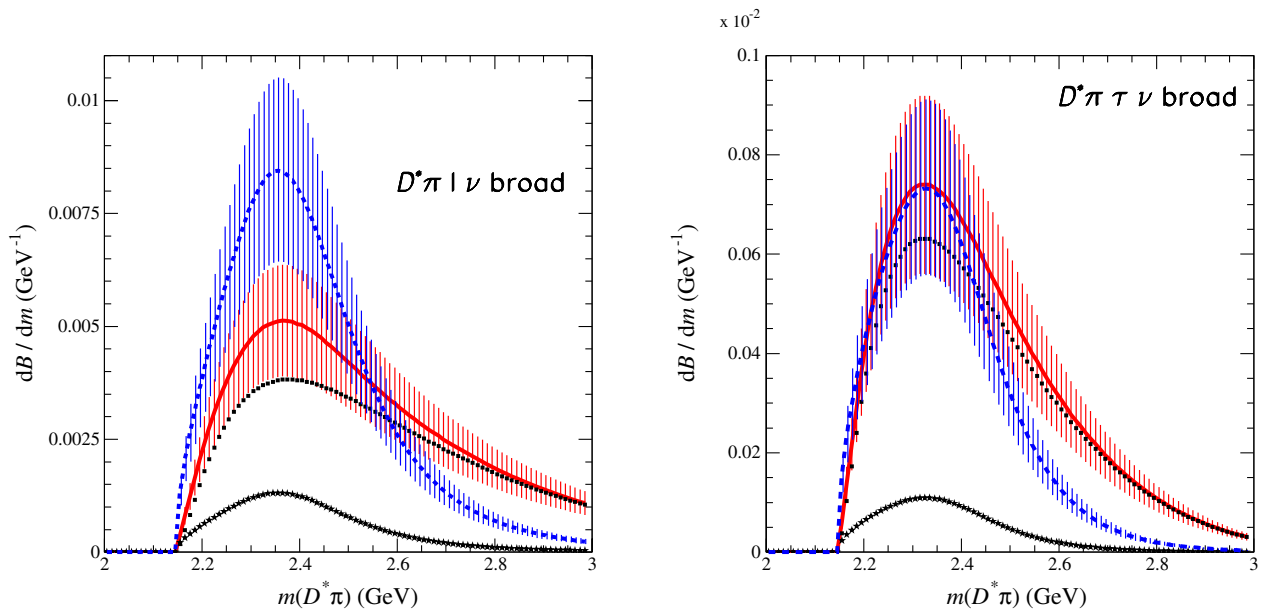


FIG. 6. Expected broad $D^*\pi$ mass distributions for $\bar{B}^0 \rightarrow D^*\pi$ in semileptonic decays. The same conventions as in Fig. 5 are used. Hatched areas include only the experimental uncertainty given in Eq. (26).

1. Expected differences between our model and LLSWBi for broad mass components

In the following we compare expected mass (Fig. 6) and q^2 (Fig. 7) distributions, for the $D^*\pi$ broad mass component in our model and in LLSWBi and after having normalized expectations to agree with the measured central value for light leptons. Hatched areas only correspond to the uncertainty quoted in Eq. (26). Therefore, they are mainly indicative and do not illustrate the uncertainty on the shape

of the distributions which come from the model dependence of the two analyses.

For τ events one expects 1.3 times more events in our analysis, whereas estimates are equal, by convention, for light leptons. This comes from the different dependence of $D_V^{(*)}$ and $D_1(2430)$ components versus q^2 . The $D_V^{(*)}$ component corresponds to a $D^*\pi$ mass distribution which can mimic a broad resonance in the absence of an analysis of the angular distribution.

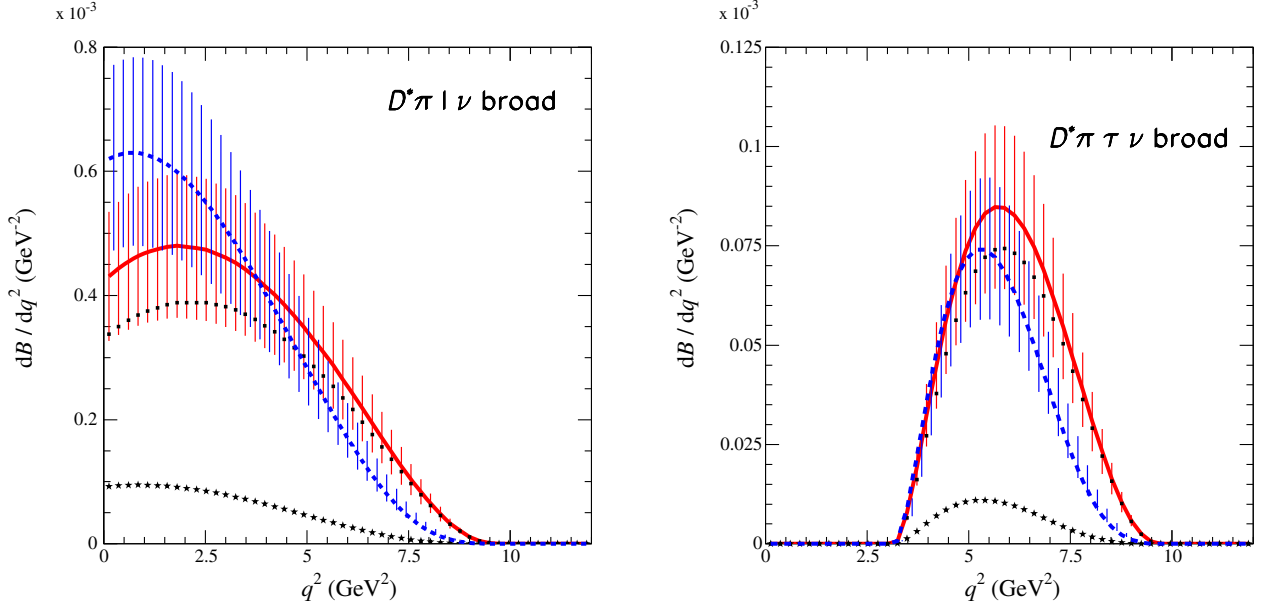


FIG. 7. Expected q^2 distributions for $\bar{B}^0 \rightarrow D^* \pi$, the broad mass component, in semileptonic decays. The same conventions as in Fig. 5 are used.

C. Analysis and predictions for the $\bar{B}^0 \rightarrow D\pi \ell^- \bar{\nu}_\ell$ final state

All quoted numbers are relative to the sum of $D^0 \pi^+$ and $D^+ \pi^0$ final states. Input measurements are given in Sec. III B 1.

The measured branching fraction into broad components amounts to

$$\mathcal{B}(\bar{B}^0 \rightarrow D\pi|_{\text{broad}} \ell^- \bar{\nu}_\ell) = (4.24 \pm 0.56) \times 10^{-3}. \quad (27)$$

In the hypothesis that contributions from higher mass resonances can be neglected, the expected contribution

from $D_{1/2}$ decays is equal to $(0.51 \pm 0.24) \times 10^{-3}$. To account for the observed broad mass $D\pi$ distribution, the $D_0(2300)^+$ contribution has to be complemented by a D_V^* component equal to $(3.7 \pm 0.6) \times 10^{-3}$. For r_{BW} values varying between 1 and 3 GeV^{-1} , our estimates are in the range $[2.6, 1.5] \times 10^{-3}$. Therefore, taking into account present uncertainties, this scenario is compatible (marginally) with present measurements.

In Fig. 8, we compare expected $D\pi$ mass distributions from our model (solid line) analysis and from the LLSWB analysis (dashed line). There is a narrow peak from the D_2^{*+} meson located on top of a broad mass distribution which is

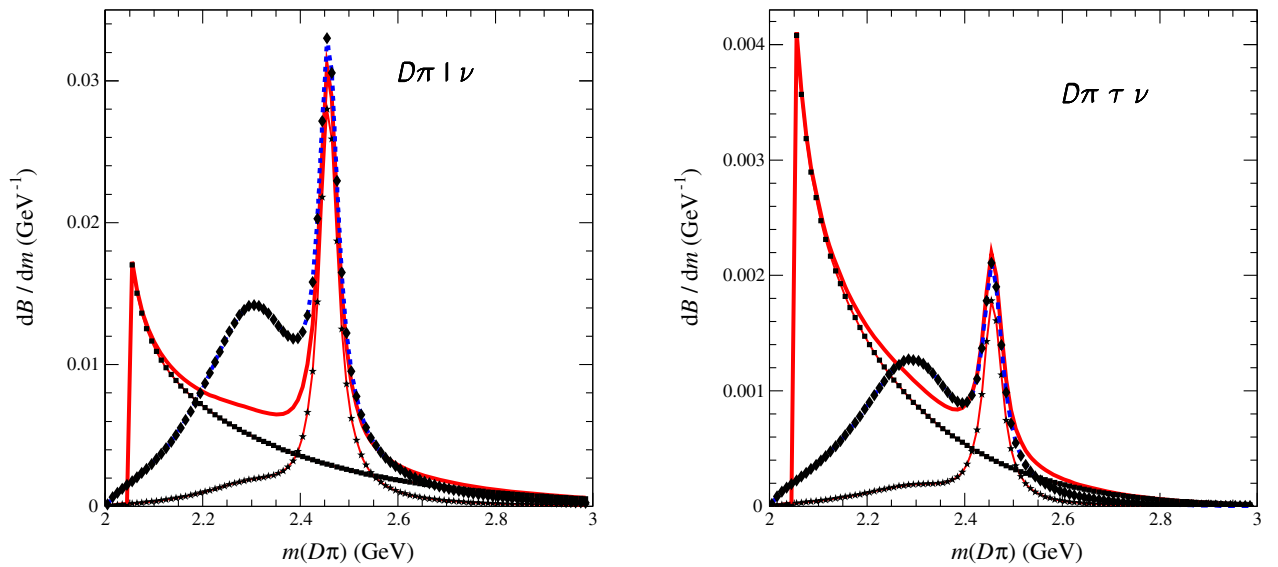


FIG. 8. Expected $D\pi$ mass distributions for $\bar{B}^0 \rightarrow D\pi$ in semileptonic decays. Only central values are displayed.

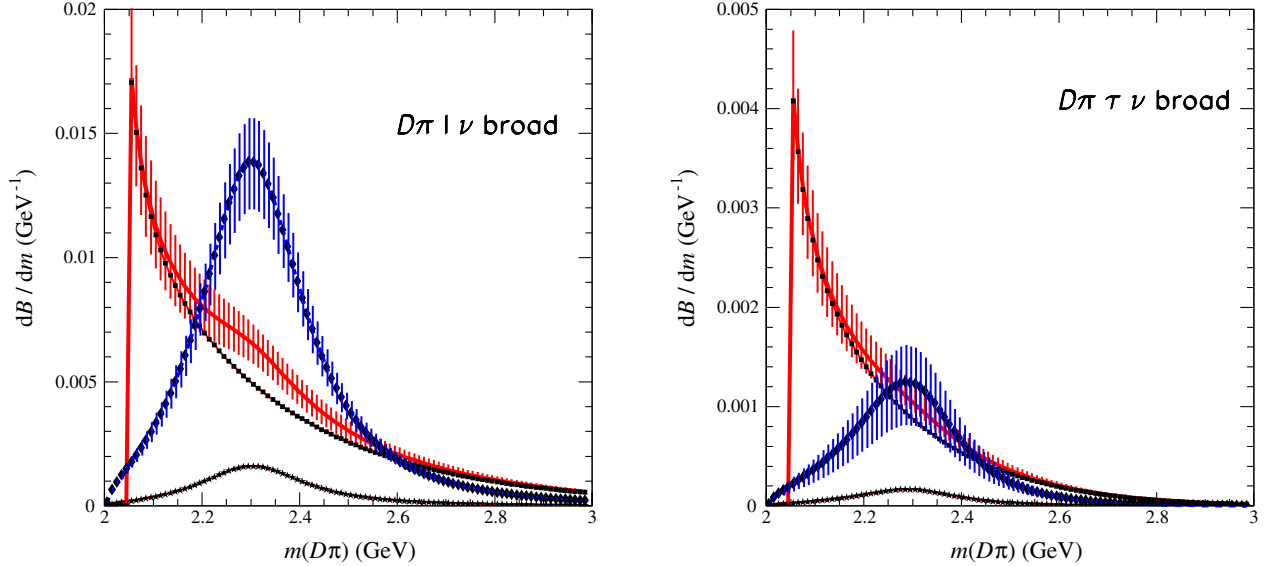


FIG. 9. Expected broad $D\pi$ mass distributions for $\bar{B}^0 \rightarrow D\pi$ in semileptonic decays.

very different in the two scenarios. As in the $D^*\pi$ channel analysis, broad mass distributions have been scaled so that total decay rates agree with measurements in the case of light leptons.

1. Expected differences between our model and LLSWBi for broad mass components

In the following we compare expected mass (Fig. 9) and q^2 (Fig. 10) distributions for the $D\pi$ broad mass component in our model and LLSWBi and after having normalized expectations to agree with the measured central value for light leptons.

Our model and LLSWBi show marked differences. In particular, for τ events one expects 2 times more candidates in our model and very different mass and q^2 distributions. Dashed areas correspond to measured uncertainties of the broad mass component, used for the normalization, as given in Eq. (27), and they do not include model uncertainties which can also affect the shape of the distributions.

X. PREDICTIONS FOR $\bar{B}^0 \rightarrow D^{**+} D_s^-$ DECAYS

We now turn to a rather different application of factorization: namely, the decay to two charmed mesons. According to BBNS (see, in particular, their Sec. 3.5.3),

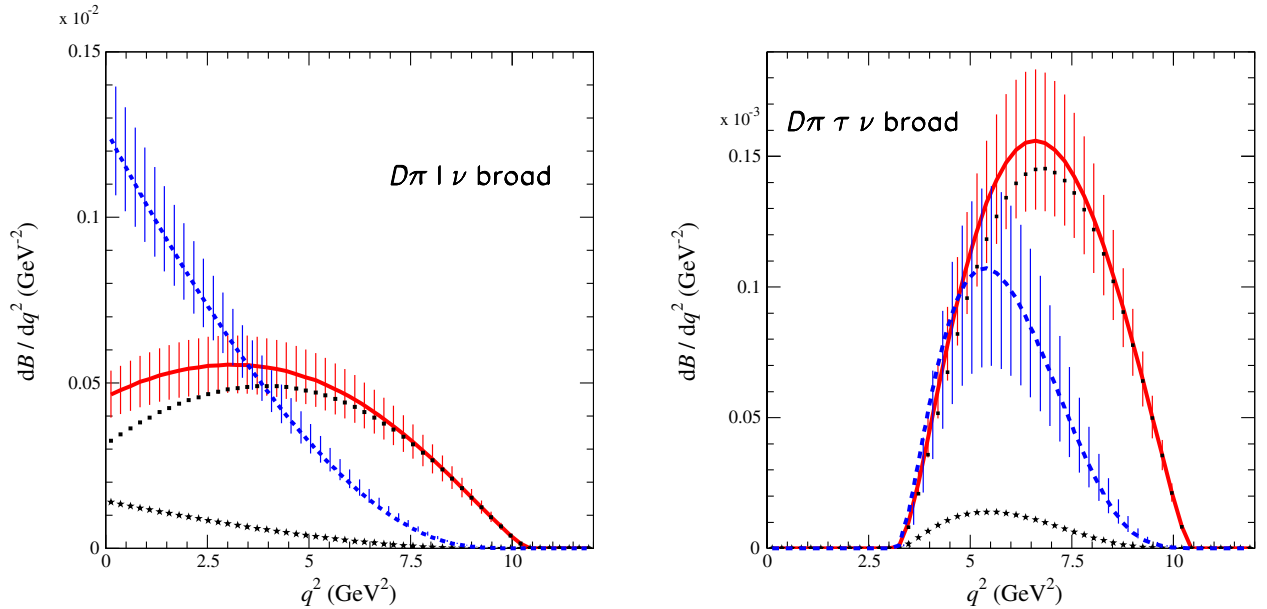


FIG. 10. Expected q^2 distributions for $\bar{B}^0 \rightarrow D\pi$, the broad mass component, in semileptonic decays.

these decays do not satisfy the conditions for QCD factorization [the QCD factorization stating that $a_1^{\text{eff}} = 1 + \mathcal{O}(\alpha_s) + \mathcal{O}(1/m_Q) + \dots$]. Therefore, they expect that instead of $\mathcal{O}(1/m_Q)$, one could have terms of order $\mathcal{O}(1/m_Q)^0$, allowing a much larger departure from 1.

However, on a purely empirical ground, using NL and SL measurements, just in the same way as for decays with a light emitted meson, we observe that factorization still holds for the transitions $\bar{B} \rightarrow D^{(*)}D_s^-$, with the same $a_{1,\text{eff}} = 0.93 \pm 0.07$, close to 1, as for pionic decays. Those reactions involve, in fact, penguin contributions. However, these contributions must be extracted to obtain a “ a_1 ” value that can be compared with the one obtained in pionic decays. This can be done by using the theoretical evaluation by Cheng and Yang [35] of the ratios $a_{1,\text{eff}}^{DD_s}/a_{1,\text{th}} = 0.847$ and $a_{1,\text{eff}}^{D^*D_s}/a_{1,\text{th}} = 1.037$. These values, which correspond to a rather large effect for the DD_s decay channel, are in agreement with the corresponding ratios we have obtained using present measurements of the different branching fractions: $a_{1,\text{eff}}^{DD_s}/a_{1,\text{exp}}^{DK} = 0.873 \pm 0.053$ and $a_{1,\text{eff}}^{D^*D_s}/a_{1,\text{exp}}^{DK} = 1.052 \pm 0.078$. Once the correcting factors are applied, one obtains $a_1^{D^{(*)}D_s}$ values very close to 0.9. To compare with theory, we have assumed that a_1 is best estimated using $\bar{B}^0 \rightarrow D^{(*)}K^-$ decays because of the absence of W -exchange amplitudes. In any case this is a small effect, and similar results are obtained when a pion is emitted in place of a kaon. Therefore, we are encouraged to extend our analysis also to transitions to $D^{**}D_s^{(*)}$, which can be easily identified and serve as an additional test of the $\tau_{1/2} \ll \tau_{3/2}$ inequality, and we give our expectations below, using the same formulas as for pionic decays, with still the same $a_{1,\text{eff}} = a_1^{D^{**}D_s} = 0.93 \pm 0.07$. Note that, in these evaluations, in the absence of explicit calculations, penguin contributions are not included for the D^{**} .

After having described our predictions for decay branching fractions of \bar{B}^0 mesons into the four $D^{**,+}$ accompanied by a D_s^- , we also give expectations for the case where one has hadronic $D^*\pi$ and $D\pi$ final states.

Because the D_s meson and the τ lepton have a similar mass, we have also evaluated [36] the ratios

$$\mathcal{R}_{D_i^{**}}^{\tau,D_s} = \frac{\mathcal{B}(\bar{B}^0 \rightarrow D_i^{**,+} \tau^- \bar{\nu}_\tau)}{\mathcal{B}(\bar{B}^0 \rightarrow D_i^{**,+} D_s^-)} \quad (28)$$

expecting that, because of correlations between the different sources of uncertainties, they are more accurate than individual measurements of the corresponding decay rates, as observed already for semileptonic channels (see Table XIII).

Results can also be used for corresponding charged B -meson decays, $B^- \rightarrow D^{**0}D_s^-$, because they are of class I (once penguin terms are neglected). Branching fractions simply have to be corrected by the ratio between charged and neutral B -meson lifetimes, and ratios $\mathcal{R}_{D_i^{**}}^{\tau,D_s}$ are the same.

A. Predicted values for $\mathcal{B}(\bar{B}^0 \rightarrow D_i^{**,+} D_s^-)$

Predicted values for $\bar{B}^0 \rightarrow D_i^{**,+} D_s^-$ decay branching fractions, in our model, are given in Table XIV.

Values obtained in the LLSWBi analysis are given in Table XIX in Appendix D 2.

Values for $D_1(2430)^+$ are very uncertain because of the lack of control of the two parameters that enter in $1/m_Q$ corrections ($\hat{\chi}_2$ and $\hat{\zeta}_1$ in the present analysis). These model uncertainties also affect the ratio $\mathcal{R}_{D_1(2430)}^{\tau,D_s}$. Measurements of nonleptonic class I B decays with $D_1(2430)$ emission are therefore desirable to improve the present situation.

To evaluate branching fractions when the hadronic final state, accompanying the D_s^- meson, is $D^*\pi$ or $D\pi$, we have

TABLE XIV. Our expectations for $\mathcal{B}(\bar{B}^0 \rightarrow D_i^{**,+} D_s^-)$ branching fractions, and their ratio, to corresponding semileptonic decays with a τ lepton. The first quoted uncertainty corresponds to the error from the fit. The model uncertainty is evaluated by changing the values of parameters that are fixed to zero by ± 0.5 GeV. Then, as explained in the text, we give indicated variations of fitted parameters which correspond to different hypotheses that enter in the parametrization of fitted expressions.

Channel	Value \pm fit	Model	HQET	IW linear	Blatt-W.
$\mathcal{B}(\bar{B}^0 \rightarrow D_2^{*+} D_s^-) \times 10^4$	5.8 ± 0.8	0.6	0.1	1.7	0.1
$\mathcal{R}_{D_2^*}^{\tau,D_s}$	0.33 ± 0.06	0.03	0.00	-0.07	0.02
$\mathcal{B}(\bar{B}^0 \rightarrow D_1^+ D_s^-) \times 10^4$	13.1 ± 3.5	0.9	-0.1	6.4	0.9
$\mathcal{R}_{D_1}^{\tau,D_s}$	0.48 ± 0.12	0.03	0.03	-0.15	-0.03
$\mathcal{B}(\bar{B}^0 \rightarrow D_0(2300)^+ D_s^-) \times 10^4$	2.3 ± 0.4	0.2	0.1	0.2	0.0
$\mathcal{R}_{D_0(2300)}^{\tau,D_s}$	0.22 ± 0.04	0.05	-0.01	0.08	-0.03
$\mathcal{B}(\bar{B}^0 \rightarrow D_1(2430)^+ D_s^-) \times 10^4$	1.4 ± 1.1	0.9	0.1	-0.1	0.0
$\mathcal{R}_{D_1(2430)}^{\tau,D_s}$	0.25 ± 0.05	$\begin{smallmatrix} +0.45 \\ -0.10 \end{smallmatrix}$	0.01	0.04	-0.03

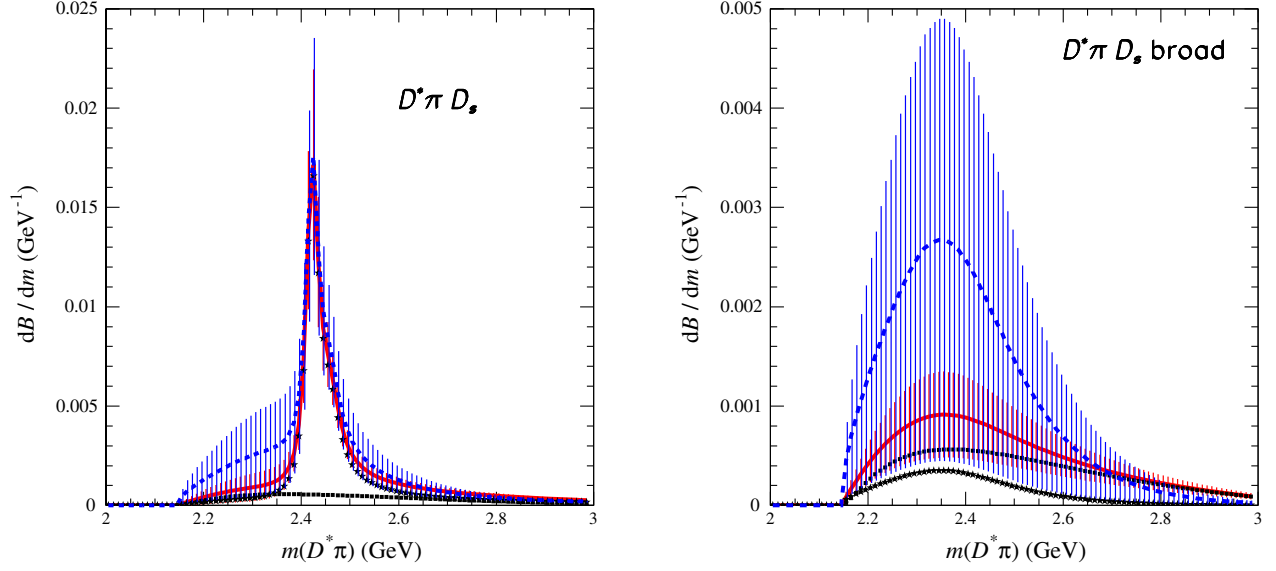


FIG. 11. Expected $D^*\pi$ mass distributions from our analysis (solid red curve) and from LLSWBi (dashed blue curve). Left plots correspond to all expected contributing components, whereas the plots on the right are for broad mass components only.

to multiply values given in Table XIV for the production of the different D_i^{**} meson by the corresponding branching fractions listed in Table VI. In our model we have also evaluated the $\bar{B}^0 \rightarrow D_V^{(*)+} D_s^-$, $D_V^{(*)+} \rightarrow D^{(*)}\pi$ expected contributions.

In practice, it is not possible to compute the expected mass distributions because of strong phase shifts between the different hadronic amplitudes, which are unknown. One can evaluate only the absolute values of these amplitudes. Therefore, mass distributions, displayed in the following, are obtained by incoherently adding individual contributing channels.

B. Analysis of the $\bar{B}^0 \rightarrow D^*\pi D_s^-$ final state

All quoted numbers are relative to the sum of $D^{*0}\pi^+$ and $D^{*+}\pi^0$ final states. Expected branching fractions for D^{**} channels, multiplied by $\mathcal{B}(D^{**} \rightarrow D^*\pi)$, are the following:

$$\begin{aligned} \mathcal{B}(\bar{B}^0 \rightarrow D_2^{*+} D_s^-) &= (2.3 \pm 0.3 \pm 0.2) \times 10^{-4} \\ \mathcal{B}(\bar{B}^0 \rightarrow D_1^+ D_s^-) &= (8.8 \pm 2.3 \pm 0.6) \times 10^{-4} \\ \mathcal{B}(\bar{B}^0 \rightarrow D_1(2430)^+ D_s^-) &= (1.4 \pm 1.1 \pm 0.9) \times 10^{-4}. \end{aligned} \quad (29)$$

To evaluate the $D^*\pi$ mass distribution (Fig. 11), D^{**} channels are complemented by the $D_V^{(*)+}$ contribution of $(3.0 \pm 1.0) \times 10^{-4}$. This gives a total broad $D^*\pi$ component of $(4.4 \pm 3.0) \times 10^{-4}$, which can be compared with the estimate from LLSWBi: $(8.8 \pm 7.4) \times 10^{-4}$.

It can be noted that the $D_V^{(*)+}$ contribution can mimic a broad resonance, and an analysis of the alignment distribution is necessary to separate the two possibilities.

C. Analysis of the $\bar{B}^0 \rightarrow D\pi D_s^-$ final state

All quoted numbers are relative to the sum of $D^0\pi^+$ and $D^+\pi^0/\gamma$ final states. Expected branching fractions for channels with a D^{**} meson, multiplied by $\mathcal{B}(D^{**} \rightarrow D\pi)$, are the following:

$$\begin{aligned} \mathcal{B}(\bar{B}^0 \rightarrow D_2^{*+} D_s^-) &= (3.48 \pm 0.46 \pm 0.33) \times 10^{-4} \\ \mathcal{B}(\bar{B}^0 \rightarrow D_0(2300)^+ D_s^-) &= (2.30 \pm 0.43 \pm 0.22) \times 10^{-4}. \end{aligned} \quad (30)$$

TABLE XV. Our expectations for $\mathcal{B}(\bar{B}^0 \rightarrow D_i^{**+} D_s^{*-})$ branching fractions, and their ratio, to corresponding semileptonic decays with a τ lepton and nonleptonic D_s^- production. The first quoted uncertainty corresponds to the error from the fit. The model uncertainty is evaluated by changing the values of the parameters that are fixed to zero by ± 0.5 GeV.

Channel	Value \pm fit	Model
$\mathcal{B}(\bar{B}^0 \rightarrow D_2^{*+} D_s^{*-}) \times 10^3$	1.9 ± 0.4	0.0
$\mathcal{R}_{D_2^*}^{\tau, D_s^*}$	0.100 ± 0.014	0.004
$\mathcal{R}_{D_2^*}^{D_s, D_s^*}$	0.30 ± 0.08	0.03
$\mathcal{B}(\bar{B}^0 \rightarrow D_1^+ D_s^{*-}) \times 10^3$	4.7 ± 0.9	0.1
$\mathcal{R}_{D_1^*}^{\tau, D_s^*}$	0.134 ± 0.024	0.0
$\mathcal{R}_{D_1^*}^{D_s, D_s^*}$	0.28 ± 0.10	0.02
$\mathcal{B}(\bar{B}^0 \rightarrow D_0(2300)^+ D_s^{*-}) \times 10^4$	2.4 ± 0.7	1.0
$\mathcal{R}_{D_0(2300)}^{\tau, D_s^*}$	0.20 ± 0.04	0.02
$\mathcal{R}_{D_0(2300)}^{D_s, D_s^*}$	0.96 ± 0.26	+0.44 -0.24
$\mathcal{B}(\bar{B}^0 \rightarrow D_1(2430)^+ D_s^{*-}) \times 10^4$	2.2 ± 2.0	+0.6 -0.1
$\mathcal{R}_{D_1(2430)}^{\tau, D_s^*}$	0.14 ± 0.02	0.02
$\mathcal{R}_{D_1(2430)}^{D_s, D_s^*}$	0.52 ± 0.02	+0.52 -0.36

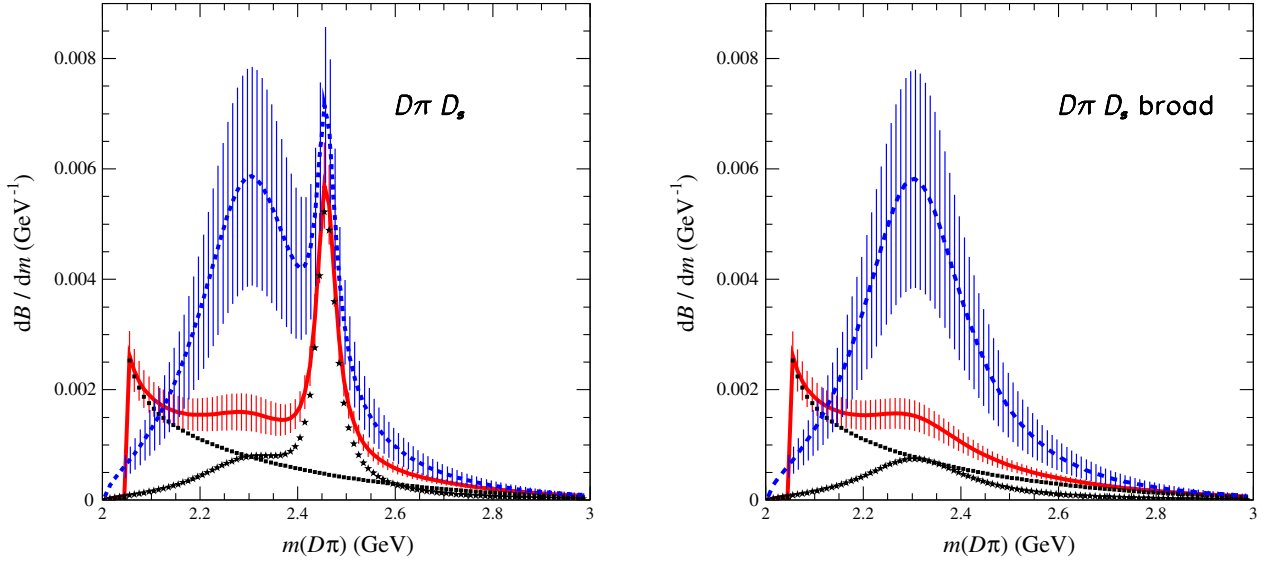


FIG. 12. Expected $D\pi$ mass distributions obtained in our model (red solid line) and in LLSWBi (blue dashed line). Left plots correspond to all expected contributing components, whereas plots on the right are for broad mass components only.

To evaluate the $D\pi$ mass distribution (Fig. 12), the D^{**} component is complemented by a D_V^* contribution evaluated to be $(5.5 \pm 0.9) \times 10^{-4}$. This gives a total broad $D\pi$ component of $(7.8 \pm 1.5) \times 10^{-4}$, which can be compared with the estimate from the LLSWBi analysis: $(17 \pm 8) \times 10^{-4}$.

XI. PREDICTIONS FOR $\bar{B}^0 \rightarrow D^{**,+} D_s^{*-}$ DECAYS

Expected results on decay branching fractions of \bar{B}^0 mesons into the four $D_i^{**,+}$ accompanied by a D_s^{*-} are given in Table XV, including different ratios that compare these branching fractions with those expected for $\bar{B}^0 \rightarrow D_i^{**,+} D_s^-$ and $\bar{B}^0 \rightarrow D_i^{**,+} \tau^- \bar{\nu}_\tau$ decays. Expressions for $\mathcal{B}(\bar{B}^0 \rightarrow D_i^{**,+} D_s^{*-})$ are given in Appendix A. They are obtained using factorization and considering only class I decay amplitudes. These expressions are valid for charged or neutral B -meson decays,

$$\mathcal{R}_{D_i^{**}}^{\tau, D_s^*} = \frac{\mathcal{B}(\bar{B}^0 \rightarrow D_i^{**,+} \tau^- \bar{\nu}_\tau)}{\mathcal{B}(\bar{B}^0 \rightarrow D_i^{**,+} D_s^{*-})} \quad (31)$$

and

$$\mathcal{R}_{D_i^{**}}^{D_s, D_s^*} = \frac{\mathcal{B}(\bar{B}^0 \rightarrow D_i^{**,+} D_s^-)}{\mathcal{B}(\bar{B}^0 \rightarrow D_i^{**,+} D_s^{*-})}. \quad (32)$$

XII. CONCLUSIONS

We have analyzed $\bar{B} \rightarrow D^{**}$ decays in semileptonic and nonleptonic class I processes that can be related using factorization.

We have verified that factorization is satisfied in $\bar{B} \rightarrow D_{3/2}$ decays and also in class I nonleptonic transitions with

D_s^- emission, with a value for a_1 similar to those measured for a D or a D^* meson.

Naturally assuming that this factorization is valid also in $\bar{B} \rightarrow D_{1/2}$ decays, one expects a quite small contribution from $D_{1/2}$ relative to $D_{3/2}$ mesons in semileptonic decays as is the case in nonleptonic class I processes. This is in contrast with the results of LLSWBi and in agreement with LQCD computations of the corresponding IW functions at maximum transfer [9] and with relativistic QM calculations [15].

To evaluate branching fractions for the different decay channels in which a D^{**} meson is produced, we use the expressions derived in [3]. They depend on several parameters that control $1/m_Q$ corrections. Using present experimental measurements and constraints from theory, we have determined the most important of these parameters for $D_{3/2}$ emission. In particular, we find that the $1/m_Q$ correction $\hat{\epsilon}_{3/2}$ included in the auxiliary $\tau_{3/2}^{\text{eff}}$ is of the order of -0.2 ± 0.1 , the minus sign confirming the agreement with a quark model calculation. The three other quantities we obtain are of the order of $\bar{\Lambda}$, as expected in a $1/m_Q$ expansion, which is encouraging in view of the roughness of the method. For $D_{1/2}$ mesons, estimates of the parameters are more uncertain, but this does not change our conclusion on the smallness of the contribution.

To explain measurements of exclusive $D^{(*)}\pi$ broad hadronic final states in B -meson semileptonic decays, we have evaluated the contribution from $D_V^{(*)}$ components, in addition to $D_{1/2}$ decays. These components can be normalized by using $\bar{B} \rightarrow D^{(*)} \ell^- \bar{\nu}_\ell$ measurements, but the mass dependence of the $D^{(*)}\pi$ mass distribution remains highly undetermined.

We propose a model that accounts for $\bar{B} \rightarrow D^{(*)}\pi\ell^-\bar{\nu}_\ell$ measurements by adding $D_V^{(*)}$ and D^{**} contributions. At present, we have not considered contributions from higher mass hadronic states. Results have been compared with the LLSWBi model in which $D_{1/2}$ mesons alone explain the broad mass spectra.

These two models give very different expectations for the broad $D^{(*)}\pi$ mass and q^2 distributions regarding light leptons. The $D\pi$ final state, in particular, can provide clear information on the relative importance of the D_V^* and $D_0(2300)$ components. The two models also have very different expectations for semileptonic decays with a τ lepton and in class I nonleptonic transitions with $D_s^{(*)}$ emission.

ACKNOWLEDGMENTS

We would like to thank colleagues who have shown interest and helped on various aspects of this analysis, namely, D. Becirevic, I. Bigi, B. Blossier, S. Descotes-Genon, and S. Fajfer. This study has been prompted by G. Wormser who asked us for some advice about measuring $\bar{B} \rightarrow D^{**}D_s^-$ decays to improve our knowledge on D^{**} production in \bar{B} decays.

APPENDIX A: EXPRESSIONS FOR CLASS I NONLEPTONIC DECAYS

Expressions for Lorentz invariant form factors are those of LLSW [3]; therefore, for the IW functions, one has to use the correspondence $\tau(w) = \sqrt{3}\tau_{3/2}(w)$ and $\zeta(w) = 2\tau_{1/2}(w)$. In following formulas, Lorentz invariant form factors are evaluated at $w_D = (m_B^2 - m_{D(V)}^2 + m_{D^{**}}^2)/(2m_B m_{D^{**}})$, while the quantity w , which appears in the rest of the expressions, is computed at the running mass value of the D^{**} resonance. Expressions for the traditional Blatt-Weisskopf damping factors in $\bar{B} \rightarrow D^{**}X$ decays, in which X is a stable particle

and which occur in an angular momentum $L = 1, 2$, and 3 , are the following:

$$\begin{aligned} F_{B,1}(p') &= \frac{1}{\sqrt{1+z}} \\ F_{B,2}(p') &= \frac{1}{\sqrt{9+3z+z^2}} \\ F_{B,3}(p') &= \frac{1}{\sqrt{225+45z+6z^2+z^3}} \end{aligned} \quad (\text{A1})$$

with $z = (r_{\text{BW}}p')^2$, in which p' is the decay momentum evaluated in the \bar{B} rest frame. For the damping term, we use $r_{\text{BW}} = 1.85 \text{ (GeV)}^{-1}$. We define the quantities

$$B_{B,L}(w) = \left(\frac{F_{B,L}(p')}{F_{B,L}(p'_0)} \right)^2 \quad (\text{A2})$$

which are the ratios of the previous functions evaluated at the running mass of the D^{**} resonance and at its nominal mass, $m_{D^{**}}$.

1. $\bar{B}^0 \rightarrow D^{**,+}P^-$ decays

We write the following expressions for a generic pseudoscalar meson denoted as “ P .” Note that $a_{1,\text{eff}}^{D_X,P}$ is an effective parameter describing the deviation from strict factorization, which also includes possible contributions from exchange, annihilation, or penguin amplitudes; $V_{q_1q_2}$ is the relevant light-quark CKM matrix element and f_P the annihilation constant. These parameters are to be adapted to the case under consideration.

The damping factor $B_{B,2}(w)$ is used for $\bar{B} \rightarrow D_{3/2}$ decays, which occur in a D -wave; as usual, no damping is considered for the decays into $D_{1/2}$ states, which are S -wave. Each expression is followed by its $m_Q = \infty$ limit (between parentheses). This is valid also in the case of a final vector meson,

$$\begin{aligned} \Gamma_{\bar{B}^0 \rightarrow D_2^{*+}P^-} &= |a_{1,\text{eff}}^{D_2^*,P}|^2 |V_{cb}V_{q_1q_2}^*|^2 \frac{G_F^2}{24\pi} f_P^2 m_B m_{D_2^*}^2 |k_{A_1} + k_{A_2}(1-rw) + k_{A_3}(w-r)|^2 (w^2-1)^{5/2} B_{B,2}(w) \\ &\quad \left(|a_{1,\text{eff}}^{D_2^*,P}|^2 |V_{cb}V_{q_1q_2}^*|^2 \frac{G_F^2}{24\pi} f_P^2 m_B m_{D_2^*}^2 \tau(w)^2 (1-r)^2 (1+w)^2 (w^2-1)^{3/2} \right), \end{aligned} \quad (\text{A3})$$

$$\begin{aligned} \Gamma_{\bar{B}^0 \rightarrow D_1^+P^-} &= |a_{1,\text{eff}}^{D_1^*,P}|^2 |V_{cb}V_{q_1q_2}^*|^2 \frac{G_F^2}{16\pi} f_P^2 m_B m_{D_1^*}^2 |f_{V_1} + f_{V_2}(1-rw) + f_{V_3}(w-r)|^2 (w^2-1)^{3/2} B_{B,2}(w) \\ &\quad \left(|a_{1,\text{eff}}^{D_1^*,P}|^2 |V_{cb}V_{q_1q_2}^*|^2 \frac{G_F^2}{24\pi} f_P^2 m_B m_{D_1^*}^2 \tau^2 (1-r)^2 (1+w)^2 (w^2-1)^{3/2} \right), \end{aligned} \quad (\text{A4})$$

$$\begin{aligned} \Gamma_{\bar{B}^0 \rightarrow D_0(2300)^+P^-} &= |a_{1,\text{eff}}^{D_0^*,P}|^2 |V_{cb}V_{q_1q_2}^*|^2 \frac{G_F^2}{16\pi} f_P^2 m_B m_{D_0^*}^2 |g_+(1-r)(1+w) + g_-(1+r)(1-w)|^2 (w^2-1)^{1/2} \\ &\quad \left(|a_{1,\text{eff}}^{D_0^*,P}|^2 |V_{cb}V_{q_1q_2}^*|^2 \frac{G_F^2}{16\pi} f_P^2 m_B m_{D_0^*}^2 \zeta^2 (1+r)^2 (1-w)^2 (w^2-1)^{1/2} \right), \end{aligned} \quad (\text{A5})$$

$$\Gamma_{\bar{B}^0 \rightarrow D_1^{*+} P^-} = |a_{1,\text{eff}}^{D_1^{*+} P^-}|^2 |V_{cb} V_{q_1 q_2}^*|^2 \frac{G_F^2}{16\pi} f_P^2 m_B m_{D_1^*}^2 (w^2 - 1)^{3/2} |g_{V1} + g_{V2}(1 - rw) + g_{V3}(w - r)|^2$$

$$\left(|a_{1,\text{eff}}^{D_1^{*+} P^-}|^2 |V_{cb} V_{q_1 q_2}^*|^2 \frac{G_F^2}{16\pi} f_P^2 m_B m_{D_1^*}^2 (1 - r)^2 \zeta^2 (w^2 - 1)^{3/2} \right). \quad (\text{A6})$$

2. $\bar{B}^0 \rightarrow D^{*+} V^-$ decays

These expressions are obtained by a direct calculation. Several partial waves contribute in each decay channel, and the appropriate Blatt and Weisskopf damping factor has to be used for each contribution. It can be identified from the power of the momentum dependence,

$$\Gamma_{\bar{B}^0 \rightarrow D_2^{*+} V^-} = |a_{1,\text{eff}}^{D_2^{*+} V^-}|^2 |V_{cb} V_{q_1 q_2}^*|^2 \frac{G_F^2}{48\pi} f_V^2 \frac{m_V^2 m_{D_2^*}^2}{m_B} (w^2 - 1)^{3/2} \left[3|k_V|^2 (w^2 - 1) B_{B,2}(w) \right.$$

$$+ |k_{A_1}|^2 \left(5B_{B,1}(w) + 2 \frac{m_B^2}{m_V^2} (w^2 - 1) B_{B,2}(w) \right) + 2|k_{A_2} + \frac{1}{r} k_{A_3}|^2 (w^2 - 1)^2 \frac{m_{D_2^*}^2}{m_V^2} B_{B,3}(w)$$

$$+ 4\text{Re} \left(k_{A_1}^* \left(k_{A_2} + \frac{1}{r} k_{A_3} \right) \right) (w^2 - 1)(w - r) \frac{m_B m_{D_2^*}}{m_V^2} \sqrt{B_{B,1}(w)} \sqrt{B_{B,3}(w)} \left. \right]$$

$$\left(|a_{1,\text{eff}}^{D_2^{*+} V^-}|^2 |V_{cb} V_{q_1 q_2}^*|^2 \frac{G_F^2}{48\pi} f_V^2 \frac{m_V^2 m_{D_2^*}^2}{m_B} \tau^2 \left(5(1 + w)^2 + (w^2 - 1) \left(3 + 4 \frac{m_B m_D}{m_V^2} (1 + w) \right) \right) (w^2 - 1)^{3/2} \right), \quad (\text{A7})$$

$$\Gamma_{\bar{B}^0 \rightarrow D_1^{*+} V^-} = |a_{1,\text{eff}}^{D_1^{*+} V^-}|^2 |V_{cb} V_{q_1 q_2}^*|^2 \frac{G_F^2}{16\pi} f_V^2 \frac{m_V^2 m_{D_1^*}^2}{m_B} (w^2 - 1)^{1/2} \left[3|f_{V_1}|^2 + (w^2 - 1) \left(|f_{V_1}|^2 \frac{m_B^2}{m_V^2} + 2|f_A|^2 \right) B_{B,1}(w) \right.$$

$$+ (w^2 - 1) B_{B,2}(w) \left(\left| f_{V_2} + \frac{1}{r} f_{V_3} \right|^2 \frac{m_{D_1^*}^2}{m_V^2} (w^2 - 1) + 2\text{Re} \left(f_{V_1}^* \left(f_{V_2} + \frac{1}{r} f_{V_3} \right) \right) (w - r) \frac{m_B m_{D_1^*}}{m_V^2} \sqrt{B_{B,1}(w)/B_{B,2}(w)} \right) \left. \right]$$

$$\left(|a_{1,\text{eff}}^{D_1^{*+} V^-}|^2 |V_{cb} V_{q_1 q_2}^*|^2 \frac{G_F^2}{96\pi} f_V^2 \frac{m_V^2 m_{D_1^*}^2}{m_B} \tau^2 \left[2(1 + w)^2 + (w^2 - 1) \left(3 + \frac{m_B^2}{m_V^2} (2r(1 + w) + 3(1 + r)^2) \right) \right] (w^2 - 1)^{3/2} \right), \quad (\text{A8})$$

$$\Gamma_{\bar{B}^0 \rightarrow D_0(2300)^+ V^-} = |a_{1,\text{eff}}^{D_0^+ V^-}|^2 |V_{cb} V_{q_1 q_2}^*|^2 \frac{G_F^2}{16\pi} f_V^2 \frac{m_{D_0^+}^4}{m_B} (w^2 - 1)^{3/2} \left| g_+ \left(1 + \frac{1}{r} \right) + g_- \left(1 - \frac{1}{r} \right) \right|^2 B_{B,1}(w)$$

$$\left(|a_{1,\text{eff}}^{D_0^+ V^-}|^2 |V_{cb} V_{q_1 q_2}^*|^2 \frac{G_F^2}{16\pi} f_V^2 m_{D_0^+}^4 / m_B \zeta^2 (1 - 1/r)^2 (w^2 - 1)^{3/2} \right), \quad (\text{A9})$$

$$\Gamma_{\bar{B}^0 \rightarrow D_1^{*+} V^-} = |a_{1,\text{eff}}^{D_1^{*+} V^-}|^2 |V_{cb} V_{q_1 q_2}^*|^2 \frac{G_F^2}{16\pi} f_V^2 \frac{m_V^2 m_{D_1^*}^2}{m_B} (w^2 - 1)^{1/2} \left[3|g_{V1}|^2 + (w^2 - 1) \left(|g_{V1}|^2 \frac{m_B^2}{m_V^2} + 2|g_A|^2 \right) B_{B,1}(w) \right.$$

$$+ (w^2 - 1) B_{B,2}(w) \left(\left| g_{V_2} + \frac{1}{r} g_{V_3} \right|^2 \frac{m_{D_1^*}^2}{m_V^2} (w^2 - 1) + 2\text{Re} \left(g_{V_1}^* \left(g_{V_2} + \frac{1}{r} g_{V_3} \right) \right) (w - r) \frac{m_B m_{D_1^*}}{m_V^2} \sqrt{B_{B,1}(w)/B_{B,2}(w)} \right) \left. \right]$$

$$\left(|a_{1,\text{eff}}^{D_1^{*+} V^-}|^2 |V_{cb} V_{q_1 q_2}^*|^2 \frac{G_F^2}{16\pi} f_V^2 m_B m_{D_1^*}^2 \zeta^2 (3(m_V/m_B)^2 (w - 1)/(w + 1) + 2((1 - r)^2 + r(1 - w))) (w^2 - 1)^{3/2} \right). \quad (\text{A10})$$

APPENDIX B: CALCULATIONS OF $\eta_{ke}^{b(c)}$ AND η^p WITH NR TREATMENT OF THE C.M. MOTION

(1) According to the standard analysis, the $\mathcal{O}(1/m_Q)$ corrections to form factors fall into two main categories, due to modifications of:

- (i) the state vectors;
- (ii) the current operators.

Here we are concerned with the first category, and the η or χ parameters precisely characterize the corrections to the form factors due to this modification of state vectors, when the current operator is kept to the infinite mass limit.

More precisely, we want to consider $\eta_{ke}^{b(c)}$, which parametrizes the effect of the kinetic operator \mathcal{O}_{ke} on,

respectively, the initial ground state and on the $j = 3/2$ final state, with specification to $w = 1$.

(2) In terms of the quark model, the modification of vector states at $w = 1$ is identified with that of the rest-frame wave functions of the mesons, and the aim is then to evaluate the effect of this modification on form factors, i.e., on matrix elements of currents when the current operator is kept to its infinite mass limit.

As concerns $\eta_{ke}^{b(c)}$, one can give an intuitive interpretation by assuming that they are generated by the addition of the heavy quark kinetic energy in the Schrödinger equation

$$p^2/2m_q \rightarrow p^2/2m_q + p^2/2m_Q$$

with m_q, m_Q being, respectively, the light and heavy quark masses. But this amounts simply to replacing m_q by the reduced mass $\mu = \frac{m_q m_Q}{m_q + m_Q}$:

$$p^2/2m_q \rightarrow p^2/2\mu.$$

This fact implies that the wave equation is the same as in the heavy quark limit, except for the change of mass. In the case of the powerlike potential r^α , this allows us to use the scale invariance to deduce the wave functions from the heavy mass limit ones ϕ^∞ , as

$$(p^2/2m_q + br^\alpha)\phi^\infty(\vec{r}) = E_n\phi^\infty(\vec{r}).$$

Performing the substitution $\vec{r} \rightarrow \lambda\vec{r}$, one has

$$\left(\frac{p^2}{2m_q\lambda^{2+\alpha}} + br^\alpha\right)\phi^\infty(\lambda\vec{r}) = \frac{E_n}{\lambda^\alpha}\phi^\infty(\lambda\vec{r}).$$

Therefore, if one chooses $\lambda = (\mu/m_q)^{1/(2+\alpha)} = (1 + (m_q/m_Q))^{-(1/(2+\alpha))}$, one sees that $\phi^\infty(\lambda\vec{r})$ is the solution of the finite mass equation. The normalized wave function is

$$\lambda^{3/2}\phi^\infty(\lambda\vec{r}).$$

Now, the NR (in fact, the familiar dipolar expression) for τ is

$$\tau(w = 1) = m(\phi_f^\infty|z|\phi_i^\infty).$$

Note that $j = 1/2$ and $j = 3/2$ are degenerate at $m_Q = \infty$ in the NR approach (no Wigner rotation) if one disregards any spin-orbit force. In fact, all the spin-dependent forces are relativistic effects in the sense that they are $\mathcal{O}(v^2/c^2)$ with respect to internal velocities. Therefore, even at finite m_Q , if one considers the fully NR approach, there are no spin-independent forces. This is what is done in the following paragraphs, where we mean only to evaluate kinetic energy corrections to B and $D^{(**)}$.

On the other hand, for η^b , which combines all the types of η relative to the B , one has to consider the spin-dependent forces since they contain the magnetic contributions generating the η 's (1,2,3). This is done below, where we use the GI model which contains all the relevant forces. An important contribution is obviously the one of spin-spin force, although it is $1/m_Q$. It lifts the degeneracy with the B^* .

We now define

$$\tau^{b,c}(w = 1) = m(\phi_f^c|z|\phi_i^b),$$

with the substitution by the finite mass wave functions, whence the corrections are represented by⁹

$$\tau^{b,c}(w = 1) - \tau(w = 1) \quad (\text{B1})$$

or, assuming the proportionality to the τ and defining reduced corrections as $\hat{\eta}$,

$$\begin{aligned} \tau^{b,c}(w = 1)/\tau(w = 1) &= 1 + \frac{\hat{\eta}_{ke}^b}{2m_b} + \frac{\hat{\eta}_{ke}^c}{2m_c} + \dots \\ &= \lambda_b^{3/2}\lambda_c^{3/2} \frac{\int d_3\vec{r}z\phi_1^\infty(\lambda_c\vec{r})\phi_0^\infty(\lambda_b\vec{r})}{\int d_3\vec{r}z\phi_1^\infty(\vec{r})\phi_0^\infty(\vec{r})} \end{aligned} \quad (\text{B2})$$

where 0,1 denote the orbital angular momentum L . If one passes to radial wave functions by means of an angular integration,

$$\tau^{b,c}(w = 1)/\tau(w = 1) = \lambda_b^{3/2}\lambda_c^{3/2} \frac{\int r^3 dr \phi_1^\infty(\lambda_c r)\phi_0^\infty(\lambda_b r)}{\int r^3 dr \phi_1^\infty(r)\phi_0^\infty(r)}.$$

If one makes $m_b = m_c = m_Q$, one finds

$$\tau^{b,c}(w = 1)/\tau(w = 1) = 1 + \frac{\hat{\eta}_{ke}^b}{2m_Q} + \frac{\hat{\eta}_{ke}^c}{2m_Q} + \dots \quad (\text{B3})$$

$$= 1/\lambda_Q = 1 + \frac{m_q/m_Q}{2 + \alpha} + \dots \quad (\text{B4})$$

$$\hat{\eta}_{ke}^b + \hat{\eta}_{ke}^c = \frac{2m_q}{2 + \alpha}. \quad (\text{B5})$$

To go further and separate $\hat{\eta}_{ke}^b$ and $\hat{\eta}_{ke}^c$, one needs explicit wave functions, which is possible for $\alpha = 2$ (harmonic oscillator) or -1 (Coulomb).

Harmonic oscillator ($\alpha = 2$): $\phi_0^\infty(r) \propto e^{-(r^2/(2R^2))}$,
 $\phi_1^\infty(r) \propto r e^{-r^2/(2R^2)}$,

⁹One must note the difference of the definitions of the Isgur-Wise functions in LLSW. This difference disappears in corrections with a hat since they represent the quotient by the Isgur-Wise functions themselves.

$$\tau^{\infty,c}(w=1)/\tau(w=1) = \left(\frac{2\lambda_c}{\lambda_c^2+1}\right)^{5/2} \quad (\text{B6})$$

whence $\hat{\eta}_{\text{ke}}^c = 0$, and $\hat{\eta}_{\text{ke}}^b = (2m_q)/(2+2) = m_q/2$.

Coulomb ($\alpha = -1$) : $\phi_0^\infty(r) \propto e^{(-r/r_0)}$, $\phi_1^\infty(r) \propto r e^{(-r/2r_0)}$,

$$\tau^{\infty,c}(w=1)/\tau(w=1) = \left(\frac{3\lambda_c^{1/2}}{\lambda_c^2+2}\right)^5 \quad (\text{B7})$$

whence $\hat{\eta}_{\text{ke}}^c = -10/6m_q$, and $\hat{\eta}_{\text{ke}}^b = (2m_q)/(2-1) + 10/6m_q = 11/3m_q$.

(3) Numerical calculation for a linear + Coulomb potential

Of course, the physical potential is rather of linear + Coulomb type. The result is expected to be between the HO and the Coulomb one. But one has no analytical solution. Therefore, we perform a numerical calculation, using the particular wave functions of Ref. [37], with a potential close to linear + Coulomb, and find, with m_Q respectively infinite or equal to 5 GeV masses (light mass: $m_q = 0.45$ GeV),¹⁰

$$\tau^{m_b=5, m_c=\infty}(w=1)/\tau(w=1) = 1 + \frac{\hat{\eta}_{\text{ke}}^b}{2m_b} = 1.053, \quad (\text{B8})$$

$$\tau^{m_b=\infty, m_c=5}(w=1)/\tau(w=1) = 1 + \frac{\hat{\eta}_{\text{ke}}^c}{2m_c} = 0.9898, \quad (\text{B9})$$

$$\begin{aligned} \tau^{m_b=5, m_c=5}(w=1)/\tau(w=1) &= 1 + \frac{\hat{\eta}_{\text{ke}}^b + \hat{\eta}_{\text{ke}}^c}{2m_Q} \\ &= 1.045, \end{aligned} \quad (\text{B10})$$

whence, approximately, $\hat{\eta}_{\text{ke}}^b \simeq 0.5$ GeV, $\hat{\eta}_{\text{ke}}^c \simeq -0.1$ GeV, which is indeed intermediate between the results from HO and Coulomb potentials. In fact, $\hat{\eta}_{\text{ke}}^b + \hat{\eta}_{\text{ke}}^c \simeq 0.5$ GeV corresponds roughly to what is expected from $\alpha = 0$ (Eq. (B5), i.e., m_q), and it is indeed well known that such a power potential $\alpha \simeq 0$ or a log one roughly approximate the linear + Coulomb one (e.g., Martin potentials).

The conclusion up to now is that $\hat{\eta}_{\text{ke}}^c < 0$. In addition, $\hat{\eta}_{\text{ke}}^b > 0$, but what must be estimated is $\hat{\eta}^b$, a common combination appearing in all the form factors, and which can therefore be interpreted as the effect of the full Lagrangian contribution; i.e., intuitively, one needs to include spin-dependent forces, which are not present in the potentials that have been considered up to now.

(4) Numerical calculation of $\hat{\eta}^b$ for the GI model.

We then consider the Godfrey and Isgur spectroscopic model with all relevant forces and, moreover, a relativistic kinetic energy. To obtain $\hat{\eta}^b$, we calculate the variation of τ with the initial B , respectively at infinite and finite mass. Finally, we find $\hat{\eta}^b \simeq -0.26$ GeV. This indicates that the effect of spin-spin force is large, dominating the kinetic energy effect.

APPENDIX C: REPEATING THE LLSWB ANALYSIS OF [4,5]

This comparison is intended to show that, using the same input data and constraints, we find, using our own code, the same values for fitted parameters as in [4,5], with the LLSWB approach.

For this purpose, measurements of B -meson semileptonic decays and $\bar{B}^0 \rightarrow D_{3/2}^+ \pi^-$ nonleptonic decays, reported in the third column of Table IV, are used to constrain parametrizations of hadronic form factors. In addition, measurements from Belle [8], which provide, respectively, four and five values for the production fractions of D_2^* and $D_0(2300)$ mesons, in different bins of the w variable are used. The w dependence of the two IW functions is assumed to be linear. The validity of factorization, with $a_1 = 1$, is assumed to relate semileptonic and nonleptonic decays in which only $D_{3/2}$ mesons are emitted.

Therefore, $\bar{B}^0 \rightarrow D_{1/2}^+ \pi^-$ nonleptonic decays are not included in the analysis. Here, D^{**} mesons are assumed to be stable (no mass distribution is considered).

We have accordingly modified our analysis, but some differences remain:

- (i) For the fractions measured in different w bins, we have not used one of the measurements in each of the two samples because these quantities are not independent (their sum is equal to 1).
- (ii) The parametrization of the different form factors is derived from the original article of [3], without using different approximations.
- (iii) In addition to α_s corrections, we have also included, for $D_{3/2}$ mesons, those at order $1/m_Q \times \alpha_s$, provided in [3].

1. Numerical aspects

Production of $D_{3/2}$ and $D_{1/2}$ mesons is evaluated separately. In addition to the normalization and slope of the IW functions, the same parameters that determine $1/m_Q$ corrections, as in [5], are fitted.

Considering $D_{3/2}$ mesons only, values of the fitted parameters are compared in Table XVI.

We obtain very similar results. The numbers of degrees of freedom differ by one unit, in the two analyses, because we have not used one of the measurements for the w dependence of D_2^* production in semileptonic decays.

¹⁰The numerical calculations can be performed for fictitious heavy quark masses because we need only the coefficient of the dependence.

TABLE XVI. Comparison between the values of fitted parameters obtained in [5] and with our own code, modified to be similar to the previous analysis and using the same input measurements.

Analysis	$\tau_{3/2}^{\text{eff}}$	$\sigma_{3/2}^2$	$\hat{\tau}_1$ (GeV)	$\hat{\tau}_2$ (GeV)	χ^2/NDF
[5]	0.40 ± 0.04	1.6 ± 0.2	-0.5 ± 0.3	2.9 ± 1.4	2.4/4
Our code	0.41 ± 0.06	1.60 ± 0.25	-0.66 ± 0.42	$5. \pm 2.$	1.8/3

TABLE XVII. Comparison between the values of fitted parameters obtained in [5] and with our own code, modified to be similar to the previous analysis. In the third line, values are obtained using the physical widths for the broad $D_{1/2}$ resonances.

Analysis	$\tau_{1/2}^{\text{eff}}$	$\sigma_{1/2}^2$	$\hat{\zeta}_1$	χ^2/NDF
[5]	0.35 ± 0.11	0.2 ± 1.4	0.6 ± 0.3	9.1/4
Our code ($\Gamma(D_{1/2}) = 0$)	0.37 ± 0.11	0.26 ± 1.23	0.23 ± 0.31	7.0/3
Our code ($\Gamma(D_{1/2}) \neq 0$)	0.30 ± 0.18	-1.6 ± 3.2	0.45 ± 0.28	6.0/3

A similar comparison is done (see Table XVII) by fitting only data relative to $D_{1/2}$ mesons, measured in semi-leptonic decays (in [5] measurements of nonleptonic transitions are not used). We have also modified our code to use the zero width formulation of our expressions as done in [5].

Very similar results are obtained in the two analyses when considering zero width resonances. In the third line, obtained using the physical resonance widths, the central value of the IW function slope is negative, which is unexpected and inconclusive because the corresponding uncertainty is large. From all fits, with or without a finite resonance width, it can be concluded that data are not able to really measure this slope.

2. Main difficulty of the LLSWB analysis

Values obtained in this way, for $\tau_{1/2}^{\text{eff}}(1)$ and $\tau_{3/2}^{\text{eff}}(1)$, are compatible. This comes simply from the fact that the measurement $\mathcal{B}(\bar{B}^0 \rightarrow D_0(2300)^+ \pi^-)$ is not included in the analyses of [4,5]. Meanwhile, expectations from relativistic quark models and LQCD [9], obtained in the $m_{b,c} \rightarrow \infty$ limit, are very different, with $\tau_{1/2}(1) \ll \tau_{3/2}(1)$.

If one assumes factorization ($a_1 = 1$), the branching fractions of the NL $\bar{B} \rightarrow D_{1/2}$ class I decays predicted in LLSWBi are, at present, higher than the measured values by at least 4 standard deviations (when including the two channels).

This is illustrated in Sec. VIII A, Table XII, where we compare expectations from our model and from the LLSWBi analysis, for nonleptonic class I $\bar{B} \rightarrow D_{1/2}$ decays.

Then, we show that it is possible to fit data in a way which satisfies factorization for narrow and broad states and which is compatible with present theoretical expectations.

APPENDIX D: SUMMARY OF HOW THE LLSWBi ANALYSIS DIFFERS FROM THE LLSWB ONE AND FROM OUR MODEL

The LLSWBi analysis uses the same hypotheses as LLSWB does, but, to make it directly comparable with our model, we use the same input measurements and the same constraints from theory, when possible.

LLSWBi differs from our model as follows:

- (i) Constraints from factorization are ignored in the production of $D_{1/2}$ mesons.
- (ii) Possible contributions from $D_V^{(*)}$ decays are ignored.
- (iii) Semileptonic branching fractions, $\mathcal{B}(\bar{B}^0 \rightarrow D_{1/2}^+ \ell^- \bar{\nu}_\ell)$, are taken from the last column of Table IV. It can be noted that the uncertainty taken for $\mathcal{B}(\bar{B}^0 \rightarrow D_1(2430)^+ \ell^- \bar{\nu}_\ell)$ is 3 times larger than the one assumed in [4,5] to account for the fact that the corresponding central value is obtained from an average of incompatible experimental results (the factor 3 is evaluated using the usual PDG recipe to scale uncertainties in this situation).
- (iv) No constraint is used on $\tau_{1/2}^{\text{eff}}$.
- (v) The measured fractions, in several w bins, attributed by Belle [8], to the $\bar{B}^0 \rightarrow D_0(2300)^+ \ell^- \bar{\nu}_\ell$ decay distribution are used.

Because LLSWBi violates factorization in $D_0(2300)$ production and theoretical expectations for $\tau_{1/2}(1)$, it cannot be considered as a possible alternative to our model. We simply mean to illustrate the large expected differences between our model and previous analyses that can be confronted with data, when available.

1. Expected values for $\mathcal{B}(\bar{B}^0 \rightarrow D_i^{**+} \ell^- \bar{\nu}_\ell)$

Expected values for semileptonic branching fractions, with a light or τ lepton, in LLSWBi, are given in

TABLE XVIII. LLSWBi model: expected semileptonic branching fractions with a light or τ lepton, and their ratio, for the individual D^{**} mesons. Only model systematic uncertainties are quoted.

Channel	e or $\mu \times 10^3$	$\tau \times 10^4$	$\mathcal{R}_{D^{**}}$ (%)
$\mathcal{B}(\bar{B}^0 \rightarrow D_2^{*+} \ell^- \bar{\nu}_\ell)$	3.16 ± 0.30	$1.90 \pm 0.27 \pm .07$	$6.01 \pm 0.49 \pm 0.19$
$\mathcal{B}(\bar{B}^0 \rightarrow D_1^+ \ell^- \bar{\nu}_\ell)$	6.40 ± 0.44	$6.19 \pm 0.56 \pm 0.15$	$9.67 \pm 0.62 \pm 0.24$
	$\times 10^4$	$\times 10^5$	(%)
$\mathcal{B}(\bar{B}^0 \rightarrow D_0(2300)^+ \ell^- \bar{\nu}_\ell)$	$39.1 \pm 7.0 \pm 0.2$	$31.9 \pm 7.9 \pm 2.0$	$8.2 \pm 1.5 \pm 0.5$
$\mathcal{B}(\bar{B}^0 \rightarrow D_1(2430)^+ \ell^- \bar{\nu}_\ell)$	$17. \pm 15. \pm 2.$	$12.8 \pm 11.5 \pm 5.0$	$7.6 \pm 1.0 \pm 2.0$

TABLE XIX. LLSWBi model: $\mathcal{B}(\bar{B}^0 \rightarrow D_i^{**,+} D_s^-)$ branching fractions, and their ratio, to corresponding semileptonic decays with a τ lepton. Only model systematic uncertainties are quoted.

Channel	Value \pm fit	Model
$\mathcal{B}(\bar{B}^0 \rightarrow D_2^{*+} D_s^-) \times 10^4$	5.7 ± 0.7	0.7
$\mathcal{R}_{D_2^*}^{\tau, D_s}$	0.34 ± 0.06	0.03
$\mathcal{B}(\bar{B}^0 \rightarrow D_1^+ D_s^-) \times 10^4$	12.3 ± 3.2	1.3
$\mathcal{R}_{D_1}^{\tau, D_s}$	0.50 ± 0.12	0.01
$\mathcal{B}(\bar{B}^0 \rightarrow D_0(2300)^+ D_s^-) \times 10^4$	16.0 ± 4.1	3.0
$\mathcal{R}_{D_0(2300)}^{\tau, D_s}$	0.20 ± 0.03	0.04
$\mathcal{B}(\bar{B}^0 \rightarrow D_1(2430)^+ D_s^-) \times 10^4$	5.3 ± 4.5	3.2
$\mathcal{R}_{D_1(2430)}^{\tau, D_s}$	0.24 ± 0.04	$^{+0.54}_{-0.12}$

Table XVIII. As expected, they differ mainly from those quoted in Table XIII on the production of $D_{1/2}$ mesons and are now similar to those obtained for $D_{3/2}$ mesons. Values obtained in this approach are essentially identical to the input values given in Table IV. Therefore, estimates for $D_1(2430)$ are quite inaccurate.

2. Expected values for $\mathcal{B}(\bar{B}^0 \rightarrow D_i^{**,+} D_s^-)$

Values for $\bar{B}^0 \rightarrow D_{3/2} D_s^-$ branching fractions are essentially identical to those obtained in our analysis. On the contrary, for $D_{1/2}$ mesons, they differ by about an order of magnitude, as expected.

-
- [1] A. K. Leibovich, Z. Ligeti, I. W. Stewart, and M. B. Wise, *Phys. Rev. Lett.* **78**, 3995 (1997).
- [2] A. Le Yaouanc, J.-P. Leroy, and P. Roudeau, *Phys. Rev. D* **99**, 073010 (2019).
- [3] A. K. Leibovich, Z. Ligeti, I. W. Stewart, and M. B. Wise, *Phys. Rev. D* **57**, 308 (1998).
- [4] F. U. Bernlochner and Z. Ligeti, *Phys. Rev. D* **95**, 014022 (2017).
- [5] F. U. Bernlochner, Z. Ligeti, and D. J. Robinson, *Phys. Rev. D* **97**, 075011 (2018).
- [6] Y. Amhis *et al.* (HFLAV Collaboration), *Eur. Phys. J. C* **81**, 226 (2021).
- [7] M. Tanabashi *et al.* (Particle Data Group), *Phys. Rev. D* **98**, 030001 (2018).
- [8] D. Liventsev *et al.* (Belle Collaboration), *Phys. Rev. D* **77**, 091503 (2008).
- [9] B. Blossier, M. Wagner, and O. Pène (European Twisted Mass Collaboration), *J. High Energy Phys.* **06** (2009) 022.
- [10] S. Godfrey and N. Isgur, *Phys. Rev. D* **32**, 189 (1985).
- [11] J. D. Bjorken, I. Dunietz, and J. Taron, *Nucl. Phys.* **371**, 111 (1992).
- [12] A. Le Yaouanc, L. Oliver, and J.-C. Raynal, *Phys. Rev. D* **69**, 094022 (2004).
- [13] N. Uraltsev, *Phys. Lett. B* **501**, 86 (2001).
- [14] N. Isgur and M. B. Wise, *Phys. Rev. D* **43**, 819 (1991).
- [15] A. Le Yaouanc, V. Morénas, L. Oliver, O. Pène, and J.-C. Raynal, *Phys. Rev. D* **56**, 5668 (1997).
- [16] I. I. Bigi, B. Blossier, A. Le Yaouanc, L. Oliver, and O. Pène, *Eur. Phys. J. C* **52**, 975 (2007).
- [17] D. Becirevic, A. Le Yaouanc, L. Oliver, J.-C. Raynal, P. Roudeau, and J. Serrano, *Phys. Rev. D* **87**, 054007 (2013).

- [18] I. Bigi, M. Shifman, N. G. Uraltsev, and A. Vainshtein, *Phys. Rev. D* **52**, 196 (1995).
- [19] P. Gambino, T. Mannel, and N. G. Uraltsev, *J. High Energy Phys.* **10** (2012) 169.
- [20] S. Veseli and M. G. Olsson, *Phys. Rev. D* **54**, 886 (1996).
- [21] M. Neubert, *Phys. Rep.* **245**, 259 (1994).
- [22] M. J. Dugan and B. Grinstein, *Phys. Lett. B* **255**, 583 (1991).
- [23] M. Beneke, G. Buchalla, M. Neubert, and C. T. Sachrajda, *Nucl. Phys.* **B591**, 313 (2000).
- [24] C. W. Bauer, D. Pirjol, and I. W. Stewart, *Phys. Rev. Lett.* **87**, 201806 (2001).
- [25] T. Huber, S. Kränkl, and X. Q. Li, *J. High Energy Phys.* **09** (2016) 112.
- [26] J. D. Bjorken, *Nucl. Phys. B, Proc. Suppl.* **11**, 325 (1989).
- [27] M. Neubert, *Phys. Lett. B* **418**, 173 (1998).
- [28] K. Abe *et al.* (Belle Collaboration), Report No. ICHEP04 11-0710.
- [29] B. Aubert *et al.* (BABAR Collaboration), *Phys. Rev. Lett.* **100**, 151802 (2008).
- [30] A. Vossen *et al.* (Belle Collaboration), *Phys. Rev. D* **98**, 012005 (2018).
- [31] J. A. Bailey *et al.* (MILC Collaboration), *Phys. Rev. D* **92**, 034506 (2015).
- [32] I. Caprini, L. Lellouch, and M. Neubert, *Nucl. Phys.* **B530**, 153 (1998).
- [33] S. Fajfer, J. F. Kamenik, and I. Nisandzic, *Phys. Rev. D* **85**, 094025 (2012).
- [34] F. Jugeau, A. Le Yaouanc, L. Oliver, and J.-C. Raynal, *Phys. Rev. D* **72**, 094010 (2005).
- [35] H.-Y. Cheng and K.-C. Yang, *Phys. Rev. D* **59**, 092004 (1999).
- [36] This study was initiated following a proposal from G. Wormser.
- [37] B. Chen, K.-W. Wei, X. Liu, and T. Matsuki, *Eur. Phys. J. C* **77**, 154 (2017).